Hyperbolic divergence cleaning in lattice Boltzmann magnetohydrodynamics

Paul J. Dellar*

OCIAM, Mathematical Institute, University of Oxford,
Radcliffe Observatory Quarter, Oxford OX2 6GG, UK

Abstract. Magnetohydrodynamics couples the Navier–Stokes and Maxwell's equations to describe the flow of electrically conducting fluids in magnetic fields. Maxwell's equations require the divergence of the magnetic field to vanish, but this condition is typically not preserved exactly by numerical algorithms. Solutions can develop artifacts because structural properties of the magnetohydrodynamic equations then fail to hold. Magnetohydrodynamics with hyperbolic divergence cleaning permits a nonzero divergence that evolves under a telegraph equation, designed to both damp the divergence, and propagate it away from any sources, such as poorly resolved regions with large spatial gradients, without significantly increasing the computational cost. We show that existing lattice Boltzmann algorithms for magnetohydrodynamics already incorporate hyperbolic divergence cleaning, though they typically use parameter values for which it reduces to parabolic divergence cleaning under a slowly-varying approximation. We recover hyperbolic divergence cleaning by adjusting the relaxation rate for the trace of the tensor that represents the electric field, and absorb the contribution from the symmetric-traceless part of this tensor using a change of variables. Numerical experiments confirm that the qualitative behaviour changes from parabolic to hyperbolic when the relaxation time for the trace of the electric field tensor is increased.

Key words: magnetohydrodynamics, divergence cleaning, telegraph equations, matrix collision operators, linear viscoelasticity

1 Introduction

Magnetohydrodynamics (MHD) describes flows of electrically conducting fluids in magnetic fields by coupling the Navier–Stokes equations with Maxwell's equations. The latter require the magnetic field to have zero divergence, but this condition is typically not preserved exactly in numerical simulations. A non-vanishing $\nabla\cdot\mathbf{B}$ can create artifacts in simulations because structural properties of the MHD equations fail to hold [1–4]. For

*Corresponding author. *Email address:* dellar@maths.ox.ac.uk (P. J. Dellar)

To appear in Communications in Computational Physics Accepted 22 September 2022

example, the divergence of the Maxwell stress $\frac{1}{2}|\mathbf{B}|^2\mathbf{I}-\mathbf{B}\mathbf{B}$ is no longer equal to minus the Lorentz force $(\nabla\times\mathbf{B})\times\mathbf{B}$, and no longer perpendicular to the magnetic field $\mathbf{B}$.

There are several approaches to resolving this problem, some inspired by earlier work on an analogous problem for the electric field $\mathbf{E}$ in electrostatically interacting systems. While $\nabla\cdot\mathbf{E}$ is generally not zero in Maxwell's equations, a consistency condition connects the evolution of $\nabla\cdot\mathbf{E}$ with the electric current $\mathbf{J}_e$. This consistency condition is usually not preserved by numerical algorithms, especially those using the "particle-in-cell" approach [5–8].

Yee's [9] finite difference time domain (FDTD) scheme for Maxwell's equations exactly preserves a particular discrete approximation to $\nabla\cdot\mathbf{B}=0$ by representing the electric and magnetic fields on a staggered grid. Evans & Hawley [10] extended this scheme to MHD with a form of artificial viscosity that they named constrained transport. DeVore [11] designed a flux corrected transport scheme with the same property, and with flux limiters to resolve discontinuous solutions of the ideal MHD equations. Tóth [3] showed that these schemes can be transformed into standard finite volume schemes on unstaggered grids. All these schemes are ancestors of more recent mimetic discretisations that ensure that the vector identity $\widetilde{\nabla}\cdot(\widetilde{\nabla}\times(\cdots))=0$ holds for consistent discrete divergence $\widetilde{\nabla}\cdot(\cdots)$ and curl $\widetilde{\nabla}\times(\cdots)$ operators [12, 13].

Brackbill & Barnes [1], and also Boris [5], proposed a projection method for evolving the magnetic field in discrete timesteps of length Δt, following the pressure projection method used for solving the incompressible Navier–Stokes equations [14–16]. In its simplest form, this projection method is:

$$\mathbf{B}^\star=\mathbf{B}^n-\Delta t(\widetilde{\nabla}\times\mathbf{E})^n, \tag{1.1a}$$

$$\mathbf{B}^{n+1}=\mathbf{B}^\star-\widetilde{\nabla}\Psi^{n+1}, \tag{1.1b}$$

where $\widetilde{\nabla}$ denotes some discrete approximation to a differential operator. The magnetic field $\mathbf{B}^n$ is evolved forwards by a single timestep to define an intermediate solution $\mathbf{B}^\star$. This intermediate solution is then projected onto the space of divergence-free vector fields by subtracting the gradient of a scalar field Ψ^{n+1} determined by solving the elliptic equation $\widetilde{\nabla}^2\Psi^{n+1}=\widetilde{\nabla}\cdot\mathbf{B}^\star$. This method ensures that $\widetilde{\nabla}\cdot\mathbf{B}^{n+1}=0$ provided the various discrete operators satisfy $\widetilde{\nabla}^2\Psi=\widetilde{\nabla}\cdot(\widetilde{\nabla}\Psi)$ [2, 3, 17].

Dedner *et al.* [18] considered a set of MHD equations based on an extended form of Maxwell's equations with [6–8]

$$\partial_t\mathbf{B}+\nabla\times\mathbf{E}+\nabla\Psi=0, \tag{1.2a}$$

$$\mathcal{D}(\Psi)+\nabla\cdot\mathbf{B}=0. \tag{1.2b}$$

The evolution equation for $\mathbf{B}$ contains an extra contribution from the gradient of a scalar field Ψ that is related to $\nabla\cdot\mathbf{B}$ by a general linear operator $\mathcal{D}$. We can interpret the projection method (1.1a,b) as a particular discretisation of (1.2a,b) with $\mathcal{D}(\Psi)=-\nabla^2\Psi$ via operator splitting. Conversely, we can interpret (1.2a,b) as a continuous-time version of

the projection method, analogous to Chorin's artificial compressibility approach for solving the incompressible Navier–Stokes equations [19]. We can also interpret (1.2a) as a Helmholtz decomposition of $\partial_t \mathbf{B}$, treated as an arbitrary vector field, into a divergence-free part $\nabla \times \mathbf{E}$ and a curl-free part $\nabla \Psi$. Following yet another approach, Assous *et al.* [6] derived (1.2a) by introducing Ψ as a field of Lagrange multipliers to enforce $\nabla \cdot \mathbf{B} = 0$ in a variational formulation of Maxwell's equations.

Choosing instead $\mathcal{D}(\Psi) = (\partial_t \Psi + (1/\tau)\Psi)/c_\Psi^2$ leads to the telegraph equation

$$\partial_{tt}(\nabla \cdot \mathbf{B}) + (1/\tau)\partial_t(\nabla \cdot \mathbf{B}) = c_\Psi^2 \nabla^2(\nabla \cdot \mathbf{B}). \tag{1.3}$$

Short wavelength disturbances in $\nabla \cdot \mathbf{B}$ propagate away from any sources with speed c_Ψ, while long wavelength disturbances decay like $\exp(-t/\tau)$. For suitable choices of τ and c_Ψ, the extended system (1.2a,b) can be solved with only a modest increase in computational cost over solving the original MHD equations. There is no need to compute the solutions of elliptic equations that are needed in the projection method. The extended system is described as the MHD equations with hyperbolic divergence cleaning, as $\nabla \cdot \mathbf{B}$ evolves according to the second-order hyperbolic equation (1.3). More recently, hyperbolic divergence cleaning has been implemented in smoothed particle magnetohydrodynamics [4, 20]. This approach naturally uses material time derivatives following fluid particles, and so replaces the partial time derivative $\partial_t \Psi$ with a material time derivative $(\partial_t + \mathbf{u} \cdot \nabla)\Psi$ following the fluid velocity $\mathbf{u}$.

The work described in this paper is inspired by recent work by Baty *et al.* [21] that extended an existing lattice Boltzmann MHD formulation [22–25] to include Ψ as an extra scalar field represented by an extra set of distribution functions. Baty *et al.* [21] also represented the fluid velocity field using a second set of vector distribution functions, the same vectorial approach used by Zhao [26] for pure hydrodynamics, rather than adapting one of the standard hydrodynamic lattice Boltzmann algorithms based on scalar distribution functions [22–25].

In this paper we show that there is no need to include Ψ as an extra degree of freedom represented by extra distribution functions. The functionality needed to simulate the system (1.2a,b) is already present in the existing lattice Boltzmann MHD formulation that evolves the magnetic field according to [22–25]

$$\partial_t \mathbf{B} + \nabla \cdot \mathbf{\Lambda} = 0, \tag{1.4}$$

where $\mathbf{\Lambda}$ is a general rank-2 tensor. This reduces to Maxwell's evolution equation for $\mathbf{B}$ if $\Lambda_{\alpha\beta} = -\epsilon_{\alpha\beta\gamma} E_\gamma$ is purely antisymmetric. However, $\mathbf{\Lambda}$ does not remain antisymmetric as it evolves (see Section 5). The trace of $\mathbf{\Lambda}$ can be used to represent the scalar field Ψ in the divergence cleaning equations.

Moreover, the underlying kinetic formulation implies that $\mathrm{Tr}\mathbf{\Lambda}$ evolves according to

$$\partial_t \mathrm{Tr}\mathbf{\Lambda} + \sum_\alpha M_{\alpha\alpha\alpha} = -\frac{1}{\tau}\mathrm{Tr}\mathbf{\Lambda}, \tag{1.5}$$

where $M_{\alpha\alpha\alpha}$ (no implied summation) are the diagonal components of a tensor $\mathbf{M}$ defined in Section 5. Approximating the components of $\mathbf{M}$ by their equilibrium values, $M^{(0)}_{\alpha\beta\gamma} = \Theta\delta_{\alpha\beta}B_\gamma$ for some constant Θ, gives (1.2a) with $\mathcal{D}(\Psi) = (\partial_t\Psi + (1/\tau)\Psi)/c_\Psi^2$ and $c_\Psi^2 = \Theta/3$. It turns out that $\nabla\cdot\mathbf{B}$ then satisfies a slight modification of (1.3), with the modification arising from the symmetric-traceless part of $\mathbf{\Lambda}$.

However, the kinetic relaxation time τ is normally sufficiently short that we can approximate (1.5) by its Chapman–Enskog expansion $\mathrm{Tr}\mathbf{\Lambda} = -\tau\Theta\nabla\cdot\mathbf{B} + O(\tau^2)$. This expansion is valid for solutions that vary slowly over timescales much longer than τ. Indeed, the whole tensor $\mathbf{\Lambda}$ is then given by $\mathbf{\Lambda} = \mathbf{u}\mathbf{B} - \mathbf{B}\mathbf{u} - \tau\Theta\nabla\mathbf{B} + O(\tau^2)$, so (1.4) becomes [22,23,25]

$$\partial_t\mathbf{B} = \nabla\times(\mathbf{u}\times\mathbf{B} - \eta\nabla\times\mathbf{B}) + \nabla(\eta\nabla\cdot\mathbf{B}). \tag{1.6}$$

This is the resistive MHD induction equation with resistivity $\eta = \tau\Theta$, and a parabolic divergence cleaning term $\nabla(\eta\nabla\cdot\mathbf{B})$ that matches the system (1.2a,b) with $\mathcal{D}(\Psi) = \Psi/\eta$.

By adapting the collision operator applied to the magnetic distribution functions we can promote $\mathrm{Tr}\mathbf{\Lambda}$ to be a freely evolving variable, rathern than a variable that is expressed in terms of $\mathbf{B}$ and its spatial derivatives by the Chapman–Enskog expansion. We then recover the hyperbolic form of divergence cleaning, just as we previously recovered Maxwell's equations instead of the MHD equations by promoting the electric field encoded in the antisymmetric part of $\mathbf{\Lambda}$ to be a freely evolving variable, rather than being expressed in terms of $\mathbf{B}$ and its gradient via Ohm's law [24].

2 Maxwell's equations and magnetohydrodynamics

Maxwell's equations govern the evolution of electric and magnetic fields. In media without significant polarisation or magnetisation effects, Maxwell's equations are [27,28]

$$\nabla\cdot\mathbf{E} = \rho_e c^2, \quad \nabla\cdot\mathbf{B} = 0, \quad \partial_t\mathbf{B} + \nabla\times\mathbf{E} = 0, \quad -(1/c^2)\partial_t\mathbf{E} + \nabla\times\mathbf{B} = \mathbf{J}_e. \tag{2.1}$$

These equations are written in units that absorb the vacuum permeability μ_0 into the electric field $\mathbf{E}$ and magnetic field $\mathbf{B}$. They support wave-like solutions that propagate with the speed of light c. In media, there are sources of electric charge ρ_e and electric current $\mathbf{J}_e$ in the equations for $\nabla\cdot\mathbf{E}$ and $\partial_t\mathbf{E}$, but no corresponding sources in the equations for $\nabla\cdot\mathbf{B}$ and $\partial_t\mathbf{B}$. The divergence of the evolution equation for $\mathbf{B}$ gives

$$\partial_t(\nabla\cdot\mathbf{B}) = -\nabla\cdot(\nabla\times\mathbf{E}) = 0, \tag{2.2}$$

since the divergence of the curl of any vector field is identically zero. Maxwell's equation $\nabla\cdot\mathbf{B} = 0$ can thus be treated as an initial condition, one that is preserved under the subsequent evolution of $\mathbf{B}$.

The equations of magnetohydrodynamics (MHD) combine Maxwell's equations with the Navier–Stokes equations to describe electrically conducting fluids coupled to magnetic fields [29]. The electric field typically scales as $|\mathbf{E}| \sim |\mathbf{u}||\mathbf{B}|$ in a fluid moving with

velocity $\mathbf{u}$. We may thus neglect Maxwell's displacement current $(-1/c^2)\partial_t\mathbf{E}$ in (2.1) for non-relativistic flows with $|\mathbf{u}| \ll c$. The electric current is then simply $\mathbf{J}_e = \nabla\times\mathbf{B}$. Moreover, the electric field is given instantaneously by Ohm's law, which in its simplest form is $\mathbf{E}+\mathbf{u}\times\mathbf{B}=\eta\nabla\times\mathbf{B}$ for resistive MHD with resistivity η. The magnetic field thus evolves according to

$$\partial_t\mathbf{B} = \nabla\times(\mathbf{u}\times\mathbf{B}-\eta\nabla\times\mathbf{B}). \tag{2.3}$$

Meanwhile, the fluid density ρ and velocity $\mathbf{u}$ evolve according to

$$\partial_t\rho+\nabla\cdot(\rho\mathbf{u})=0, \quad \partial_t(\rho\mathbf{u})+\nabla\cdot(\rho\mathbf{u}\mathbf{u})+\nabla p=\nabla\cdot(\mu\mathbf{e})+\mathbf{J}_e\times\mathbf{B}, \tag{2.4}$$

where $\mathbf{e}=\nabla\mathbf{u}+(\nabla\mathbf{u})^\mathsf{T}$ is the symmetrised velocity gradient tensor, and μ is the dynamic viscosity of the fluid. There is an extra Lorentz force $\mathbf{J}_e\times\mathbf{B}$ on the right hand side of the momentum equation. Using $\nabla\cdot\mathbf{B}=0$, we can rewrite the momentum equation in conservation form as

$$\partial_t(\rho\mathbf{u})+\nabla\cdot\left(\rho\mathbf{u}\mathbf{u}+p\mathbf{I}-\mu\mathbf{e}+\tfrac{1}{2}|\mathbf{B}|^2\mathbf{I}-\mathbf{B}\mathbf{B}\right)=0. \tag{2.5}$$

The tensor $\frac{1}{2}|\mathbf{B}|^2\mathbf{I}-\mathbf{B}\mathbf{B}$ is the Maxwell stress tensor for the magnetic field [27,28]. It comprises an isotropic magnetic pressure $\frac{1}{2}|\mathbf{B}|^2$ that augments the fluid pressure p, and a magnetic tension $\mathbf{B}\mathbf{B}$ in the direction of the magnetic field.

3 Extended Maxwell equations for divergence cleaning

The Maxwell equations with no sources that govern electric and magnetic fields in vacuum are invariant under duality rotations that transform $\mathbf{E}$ and $\mathbf{B}$ into [28,30,31]

$$\mathbf{E}' = \mathbf{E}\cos\varphi+c\mathbf{B}\sin\varphi, \quad \mathbf{B}' = \mathbf{B}\cos\varphi-\frac{1}{c}\mathbf{E}\sin\varphi, \tag{3.1}$$

with a constant angle φ. It is natural to consider an extended set of Maxwell equations that remains invariant under these duality rotations in the presence of sources by introducing a magnetic charge ρ_m and a magnetic current $\mathbf{J}_m$ [28,30,31]

$$\nabla\cdot\mathbf{E}=\rho_e c^2, \quad \nabla\cdot\mathbf{B}=\rho_m, \quad \partial_t\mathbf{B}+\nabla\times\mathbf{E}=-\mathbf{J}_m, \quad -\frac{1}{c^2}\partial_t\mathbf{E}+\nabla\times\mathbf{B}=\mathbf{J}_e. \tag{3.2}$$

These extended Maxwell equations contain the original Maxwell equations (2.1) as a special case when ρ_m and $\mathbf{J}_m$ vanish. By cross-differentiating (3.2) we can derive the two charge evolution equations

$$\partial_t\rho_e+c^2\nabla\cdot\mathbf{J}_e=0, \quad \partial_t\rho_m+\nabla\cdot\mathbf{J}_m=0. \tag{3.3}$$

The first of these is the consistency condition between $\nabla\cdot\mathbf{E}$ and $\mathbf{J}_e$ mentioned in the Introduction. The asymmetry in the factors of c arises from our use of the electric and

magnetic units conventionally used in MHD. The electric field in a frame moving with velocity $\mathbf{u}$ is $\mathbf{E}+\mathbf{u}\times\mathbf{B}$ with no factor of c in these units.

To derive a closed set of equations, we must relate the magnetic current vector $\mathbf{J}_m$ to the scalar magnetic charge ρ_m. The approach used by Powell [32,33] for MHD brings in the fluid velocity vector $\mathbf{u}$ to set $\mathbf{J}_m = \mathbf{u}\rho_m = \mathbf{u}\nabla\cdot\mathbf{B}$. We then obtain

$$\partial_t\mathbf{B}+\nabla\times\mathbf{E}+\mathbf{u}\nabla\cdot\mathbf{B}=0, \tag{3.4}$$

which implies

$$\partial_t(\nabla\cdot\mathbf{B})+\nabla\cdot(\mathbf{u}\nabla\cdot\mathbf{B})=0. \tag{3.5}$$

The magnetic charge density is thus transported with the fluid velocity $\mathbf{u}$. The same extension was previously introduced by Godunov [34] to transform the MHD equations into a symmetric hyperbolic system. This extension also restores Galilean invariance to the MHD equations when $\nabla\cdot\mathbf{B}\neq 0$. The associated Riemann problem contains an "8th wave" that advects $\nabla\cdot\mathbf{B}$ with the fluid velocity normal to the interface.

Dedner *et al.* [18] followed an alternative approach that does not bring in another vector field such as the fluid velocity. They set $\mathbf{J}_m = \nabla\Psi$, using the gradient operator to convert a scalar field to a vector field, and they related the new scalar field Ψ to the magnetic charge density $\nabla\cdot\mathbf{B}$ through a scalar differential operator $\mathcal{D}$ to form the system (1.2a,b).

Replacing $\mathbf{E}$ in (1.2a) using Ohm's law gives a complete set of extended MHD equations with hyperbolic divergence cleaning:

$$\partial_t\rho+\nabla\cdot(\rho\mathbf{u})=0, \tag{3.6a}$$

$$\partial_t(\rho\mathbf{u})+\nabla\cdot\left(\rho\mathbf{u}\mathbf{u}+p\mathbf{I}-\mu\mathbf{e}+\tfrac{1}{2}|\mathbf{B}|^2\mathbf{I}-\mathbf{B}\mathbf{B}\right)=0, \tag{3.6b}$$

$$\partial_t\mathbf{B}-\nabla\times(\mathbf{u}\times\mathbf{B}-\eta\nabla\times\mathbf{B})+\nabla\Psi=0, \tag{3.6c}$$

$$\alpha\partial_t\Psi+\beta\Psi+\nabla\cdot\mathbf{B}=0. \tag{3.6d}$$

We have chosen to retain the momentum equation (2.5) written in conservation form using the Maxwell stress, even though it now differs by $\mathbf{B}\nabla\cdot\mathbf{B}$ from the momentum equation (2.4) written using the Lorentz force $(\nabla\times\mathbf{B})\times\mathbf{B}$.

We now turn to a numerical implementation of this system using the lattice Boltzmann method.

4 Lattice Boltzmann hydrodynamics

The lattice Boltzmann approach embeds the target system of partial differential equations to be solved into a larger linear constant-coefficient hyperbolic system in which all nonlinearity is confined to algebraic source terms [35–37]. In particular, to simulate fluid

dynamics, the fluid density ρ, fluid velocity $\mathbf{u}$, and momentum flux $\mathbf{\Pi}$ are expressed as moments of a discrete set of scalar distribution functions $f_i(\mathbf{x},t)$,

$$\rho = \sum_{i=0}^{N} f_i, \quad \rho\mathbf{u} = \sum_{i=0}^{N} \boldsymbol{\xi}_i f_i, \quad \mathbf{\Pi} = \sum_{i=0}^{N} \boldsymbol{\xi}_i \boldsymbol{\xi}_i f_i. \tag{4.1}$$

The f_i are postulated to evolve according to a discrete velocity Boltzmann equation,

$$\partial_t f_i + \boldsymbol{\xi}_i \cdot \nabla f_i = -\sum_{j=0}^{N} \Omega_{ij} \left(f_j - f_j^{(0)} \right). \tag{4.2}$$

The left hand side represents advection of each f_i along a straight characteristic with constant velocity $\boldsymbol{\xi}_i$. The right-hand side represents a general linear collision operator that relaxes the f_i towards some equilibrium values $f_i^{(0)}$ at rates determined by the elements Ω_{ij} of a constant relaxation matrix $\mathbf{\Omega}$. The $f_i^{(0)}$ are prescribed functions of the fluid density and velocity. A common choice is [35]

$$f_i^{(0)} = w_i \rho \left\{ 1 + 3\mathbf{u}\cdot\boldsymbol{\xi}_i + \frac{9}{2}\left((\boldsymbol{\xi}_i \cdot \mathbf{u})^2 - \frac{1}{3}|\mathbf{u}|^2 \right) \right\}, \tag{4.3}$$

with the weights $w_0 = 4/9$, $w_{1,2,3,4} = 1/9$ and $w_{5,6,7,8} = 1/36$ in two dimensions. The corresponding nine discrete velocities $\boldsymbol{\xi}_i$ are shown in Fig. 1. By integrating the combination (4.2) and (4.3) along their characteristics for a timestep Δt, and making a suitable change of variables, we can derive the lattice Boltzmann equation [38, 39]

$$\overline{f}_i(\mathbf{x} + \boldsymbol{\xi}_i \Delta t, t + \Delta t) = \overline{f}_i(\mathbf{x},t) - \Delta t \sum_{j=0}^{N} \overline{\Omega}_{ij} \left(\overline{f}_j - f_j^{(0)} \right), \tag{4.4}$$

for the transformed variables

$$\overline{f}_i(\mathbf{x},t) = f(\mathbf{x},t) + \frac{1}{2}\Delta t \sum_{j=0}^{N} \Omega_{ij} \left(f_j(\mathbf{x},t) - f_j^{(0)}(\mathbf{x},t) \right). \tag{4.5}$$

The right-hand side of (4.4) contains the elements $\overline{\Omega}_{ij}$ of a transformed relaxation matrix $\overline{\mathbf{\Omega}} = \mathbf{\Omega}(\mathbf{I} + \mathbf{\Omega}\Delta t/2)^{-1}$. Due to these transformations, the discrete system (4.4) for evolving (4.5) approximates the discrete Boltzmann equation (4.2) with second-order accuracy in Δt. For the widely-used single-relaxation-time or Bhatnagar–Gross–Krook (BGK) [40] collision operator with $\mathbf{\Omega} = (1/\tau)\mathbf{I}$, this transformation gives $\overline{\mathbf{\Omega}} = 1/(\tau + \Delta t/2)\mathbf{I}$. This corresponds to the Hénon correction [41] of the relaxation time from τ in the differential equation (4.2) to $\tau + \Delta t/2$ in the discrete system (4.4). The same formulation can be derived by combining solutions of the separate advective and algebraic parts of (4.2) using Strang splitting [42, 43].

More generally, the matrix elements Ω_{ij} should be chosen so that $\mathbf{\Pi}$ is an eigenvector of $\mathbf{\Omega}$ with eigenvalue $-1/\tau$, while ρ and $\rho\mathbf{u}$ are also eigenvectors of $\mathbf{\Omega}$. The eigenvalues for ρ and $\rho\mathbf{u}$ are irrelevant because the equilibria (4.3) are constructed so that

$$\sum_{i=0}^{N} f_i^{(0)} = \rho, \quad \sum_{i=0}^{N} \boldsymbol{\xi}_i f_i^{(0)} = \rho\mathbf{u}. \tag{4.6}$$

By taking moments of (4.2) we can then derive macroscopic mass and momentum conservation equations,

$$\partial_t \rho + \nabla\cdot(\rho\mathbf{u}) = 0, \quad \partial_r(\rho\mathbf{u}) + \nabla\cdot\mathbf{\Pi} = 0, \tag{4.7}$$

with the right-hand sides vanishing, and an evolution equation for $\mathbf{\Pi}$ of the form

$$\partial_t \mathbf{\Pi} + \nabla\cdot\left(\sum_{i=0}^{N} \boldsymbol{\xi}_i\boldsymbol{\xi}_i\boldsymbol{\xi}_i f_i\right) = -\frac{1}{\tau}\left(\mathbf{\Pi} - \mathbf{\Pi}^{(0)}\right). \tag{4.8}$$

The momentum flux corresponding to the equilibria (4.3) is

$$\mathbf{\Pi}^{(0)} = \sum_{i=0}^{N} \boldsymbol{\xi}_i\boldsymbol{\xi}_i f_i^{(0)} = \theta\rho\mathbf{I} + \rho\mathbf{u}\,\mathbf{u}, \tag{4.9}$$

with constant temperature $\theta = 1/3$ in so-called lattice units for which the components of the discrete velocities $\boldsymbol{\xi}_i$ take values in $\{-1,0,1\}$. Substituting $\mathbf{\Pi} = \mathbf{\Pi}^{(0)}$ in (4.7) thus yields the compressible Euler equations with the isothermal equation of state $p = \theta\rho$.

To recover the Navier–Stokes equations, we pose a multiple-scales expansion of the f_i and the time derivative ∂_t in powers of the small parameter $\epsilon = \tau/T$, where τ is the momentum flux relaxation time in (4.8), and T is the much longer timescale on which ρ and $\mathbf{u}$ evolve. We impose solvability conditions on the expansion of the f_i that are equivalent to leaving ρ and $\mathbf{u}$, the variables preserved under relaxation, unexpanded, while expanding the momentum flux as $\mathbf{\Pi} = \mathbf{\Pi}^{(0)} + \mathbf{\Pi}^{(1)} + \cdots$. This is a more modern form of the original Chapman–Enskog expansion.

The multiple-scales expansion allows us to evaluate $\partial_{t_0}\mathbf{\Pi}^{(0)}$ in the leading-order evolution equation

$$\partial_{t_0}\mathbf{\Pi}^{(0)} + \nabla\cdot\left(\sum_{i=0}^{N} \boldsymbol{\xi}_i\boldsymbol{\xi}_i\boldsymbol{\xi}_i f_i^{(0)}\right) = -\frac{1}{\tau}\mathbf{\Pi}^{(1)}, \tag{4.10}$$

and hence express $\mathbf{\Pi}^{(1)}$ solely in terms of ρ, $\mathbf{u}$ and their spatial derivatives:

$$\mathbf{\Pi}^{(1)} = -\tau\rho\theta\left((\nabla\mathbf{u}) + (\nabla\mathbf{u})^{\mathsf{T}}\right) + \tau\nabla\cdot(\rho\mathbf{u}\mathbf{u}\mathbf{u}). \tag{4.11}$$

We thus recover the Navier–Stokes viscous stress with dynamic viscosity $\mu = \tau\rho\theta$, and an error term $\tau\nabla\cdot(\rho\mathbf{u}\mathbf{u}\mathbf{u})$ [44, 45]. The error term is smaller than the viscous stress by the square of the Mach number $\mathrm{Ma} = |\mathbf{u}|/\theta^{1/2}$. The error term arises from using the discrete

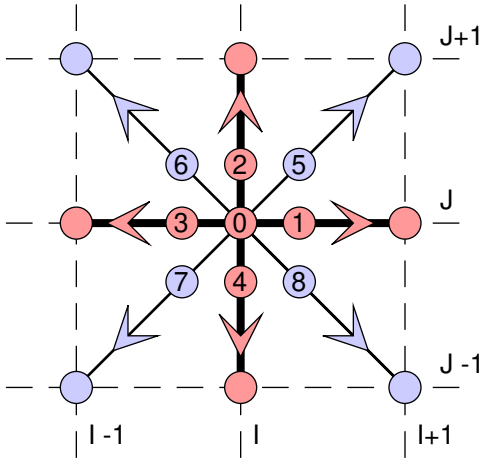

Figure 1: The nine discrete velocities $\xi_0,\ldots,\xi_8$ forming the D2Q9 lattices used for the f_i. The five discrete velocities $\xi_0,\ldots,\xi_4$ (thicker lines) form the D2Q5 lattice used for the $\mathbf{g}_i$.

equilibria (4.3) that are quadratic polynomials in the fluid velocity $\mathbf{u}$. The equivalent calculation using the true Maxwell–Boltzmann distribution from continuous kinetic theory would yield the Navier–Stokes viscous stress with no error term. The error is typically negligible in simulations with small Mach numbers that are intended to approximate incompressible flows.

5 Lattice Boltzmann magnetohydrodynamics

Using the conservation form of the momentum equation including the Maxwell stress due to the magnetic field, we can include the Lorentz force in our lattice Boltzmann formulation simply by changing the equilibrium momentum flux to be

$$\mathbf{\Pi}^{(0)} = \theta\rho\mathbf{I} + \rho\mathbf{u}\mathbf{u} + \tfrac{1}{2}|\mathbf{B}|^2\mathbf{I} - \mathbf{B}\mathbf{B}, \tag{5.1}$$

and changing the $f_i^{(0)}$ accordingly to

$$f_i^{(0)} = w_i\left[\rho\left(2 - \frac{3}{2}|\boldsymbol{\xi}_i|^2\right) + 3\rho\mathbf{u}\cdot\boldsymbol{\xi}_i + \frac{9}{2}\mathbf{\Pi}^{(0)} : \boldsymbol{\xi}_i\boldsymbol{\xi}_i - \frac{3}{2}\mathrm{Tr}\mathbf{\Pi}^{(0)}\right] \tag{5.2}$$

in two dimensions, and by a similar formula in three dimensions. The difference arises because $\mathrm{Tr}\mathbf{I} = D$, the number of spatial dimensions.

The evolution equation for the magnetic field $\mathbf{B}$ is less straightforward to simulate using a kinetic formulation. We can rewrite Maxwell's equation $\partial_t\mathbf{B} + \nabla\times\mathbf{E} = 0$ in divergence form as

$$\partial_t\mathbf{B} + \nabla\cdot\mathbf{\Lambda} = 0 \tag{5.3}$$

by introducing a tensor $\mathbf{\Lambda}$ with components $\Lambda_{\alpha\beta} = -\epsilon_{\alpha\beta\gamma} E_\gamma$. This now resembles the momentum equation (4.7), except the momentum flux tensor $\mathbf{\Pi}$ defined in (4.1) is symmetric by construction, while the electric field tensor $\mathbf{\Lambda}$ is antisymmetric by construction. It is thus impossible to recover (5.3) by representing $\mathbf{B}$ as the first moment of some scalar distribution functions, analogous to our representation of the momentum vector $\rho\mathbf{u}$ in (4.1).

Instead, we introduce a set of vector-valued distribution functions $\mathbf{g}_i(\mathbf{x},t)$, and represent $\mathbf{B}$ and $\mathbf{\Lambda}$ by

$$\mathbf{B} = \sum_{i=0}^{M} \mathbf{g}_i, \quad \mathbf{\Lambda} = \sum_{i=0}^{M} \boldsymbol{\xi}_i \mathbf{g}_i. \tag{5.4}$$

This representation of $\mathbf{\Lambda}$ is not constrained to be either symmetric or antisymmetric. We can typically choose M smaller than N, and so use fewer discrete velocities to represent the magnetic field than we used in Section 4 to represent the hydrodynamic variables. For example, in two dimensions it suffices to use just the five discrete velocities $\boldsymbol{\xi}_0,\ldots,\boldsymbol{\xi}_4$ shown in Fig. 1.

We now postulate that the $\mathbf{g}_i$ evolve according to a kinetic equation of the form

$$\partial_t \mathbf{g}_i + \boldsymbol{\xi}_i \cdot \nabla \mathbf{g}_i = -\sum_{j=0}^{M} \mathbf{L}_{ij} \left(\mathbf{g}_j - \mathbf{g}_j^{(0)} \right), \tag{5.5}$$

inspired by extending (4.2) to vector-valued distribution functions. Each element $\mathbf{L}_{ij}$ is itself a $D \times D$ matrix because $\mathbf{g}_i$ and $\mathbf{g}_j$ are D-component vectors in D spatial dimensions.

We choose the equilibrium distributions

$$\mathbf{g}_i^{(0)} = W_i \left(\mathbf{B} + \Theta^{-1} \boldsymbol{\xi}_i \cdot \mathbf{\Lambda}^{(0)} \right) \text{ with } \mathbf{\Lambda}^{(0)} = \mathbf{u}\mathbf{B} - \mathbf{B}\mathbf{u}, \tag{5.6}$$

for suitable weights W_i, and a lattice constant Θ defined by the isotropy condition

$$\sum_{j=0}^{M} W_i \boldsymbol{\xi}_i \boldsymbol{\xi}_i = \Theta \mathbf{I}. \tag{5.7}$$

In two dimensions, we take $W_0 = 1/3$ and $W_{1,2,3,4} = 1/6$, giving $\Theta = 1/3$.

Equation (5.5) implies that $\mathbf{\Lambda}$ evolves according to

$$\partial_t \mathbf{\Lambda} + \nabla \cdot \mathbf{M} = -\sum_{i=0}^{M} \boldsymbol{\xi}_i \sum_{j=0}^{M} \mathbf{L}_{ij} \left(\mathbf{g}_j - \mathbf{g}_j^{(0)} \right), \tag{5.8}$$

involving the divergence of a further tensor

$$\mathbf{M} = \sum_{i=0}^{M} \boldsymbol{\xi}_i \boldsymbol{\xi}_i \mathbf{g}_i. \tag{5.9}$$

At equilibrium, with $\mathbf{g}_i = \mathbf{g}_i^{(0)}$, the components of $\mathbf{M}$ take the values $M^{(0)}_{\alpha\beta\gamma} = \Theta\delta_{\alpha\beta}B_\gamma$.

As in our previous derivation of the Navier–Stokes equations in Section 4, we now pose a multiple-scales expansion

$$\partial_t = \partial_{t_0} + \partial_{t_1} + \cdots, \quad \mathbf{\Lambda} = \mathbf{\Lambda}^{(0)} + \mathbf{\Lambda}^{(1)} + \cdots, \quad \mathbf{M} = \mathbf{M}^{(0)} + \mathbf{M}^{(1)} + \cdots, \tag{5.10}$$

while leaving $\mathbf{B}$ unexpanded. We choose the matrix elements $\mathbf{L}_{ij}$ so that we can express the right-hand side of (5.8) as a linear operator L acting on $\mathbf{\Lambda}$, giving

$$\partial_{t_0}\mathbf{\Lambda}^{(0)} + \nabla\cdot\mathbf{M}^{(0)} = -\sum_{i=0}^{M}\xi_i\sum_{j=0}^{M}\mathbf{L}_{ij}\mathbf{g}_j^{(1)} = -\mathsf{L}\mathbf{\Lambda}^{(1)}. \tag{5.11}$$

For the simplest case with $\mathbf{L}_{ij} = (1/\tau_{\mathbf{\Lambda}})\mathbf{I}\delta_{ij}$, we thus obtain [22]

$$\mathbf{\Lambda}^{(1)} = -\tau_{\mathbf{\Lambda}}\Theta\nabla\mathbf{B} + O(|\mathbf{u}|^3). \tag{5.12}$$

The error term is $O(|\mathbf{u}|^3)$, comparable to the error in $\mathbf{\Pi}^{(1)}$, if we take the magnetic field strength to be such that the Alfvén velocity $\mathbf{B}\rho^{-1/2}$ is comparable with, or smaller than, the fluid velocity.

The evolution equation for $\mathbf{B}$ that we obtain at this order is thus

$$\partial_t\mathbf{B} = -\nabla\cdot(\mathbf{\Pi}^{(0)} + \mathbf{\Pi}^{(1)}) = -\nabla\cdot(\mathbf{u}\mathbf{B} - \mathbf{B}\mathbf{u} - \eta\nabla\mathbf{B}), \tag{5.13}$$

which rearranges into

$$\partial_t\mathbf{B} = \nabla\times(\mathbf{u}\times\mathbf{B} - \eta\nabla\times\mathbf{B}) + \nabla(\eta\nabla\cdot\mathbf{B}). \tag{5.14}$$

This is the resistive MHD induction equation in the form (1.6) with resistivity $\eta = \tau_{\mathbf{\Lambda}}\Theta$, and a parabolic divergence-cleaning term $\nabla(\eta\nabla\cdot\mathbf{B})$ from the symmetric part of $\mathbf{\Lambda}^{(1)}$.

More generally, we can specify the matrices $\mathbf{L}_{ij}$ by specifying how the right-hand side of (5.5) should act on a basis of moments of the $\mathbf{g}_i$. If we choose the 5 discrete velocites show in Fig. 1 in two dimensions, or the analogous set of 7 discrete velocities in three dimensions, then

$$B_\alpha = \sum_{i=0}^{M} g_{i\alpha}, \quad \Lambda_{\alpha\beta} = \sum_{i=0}^{M}\xi_{i\alpha}g_{i\beta}, \quad M_{\alpha\beta\gamma} = \sum_{i=0}^{M}\xi_{i\alpha}\xi_{i\beta}g_{i\gamma} \tag{5.15}$$

form a basis of moments of the $\mathbf{g}_i$. For these sets of discrete velocities, the components of $M_{\alpha\beta\gamma}$ are identically zero unless $\alpha = \beta$. There are thus D degrees of freedom in $\mathbf{B}$, and D^2 in each of $\mathbf{\Lambda}$ and $\mathbf{M}$, giving $2D^2 + D$ degrees of freedom overall.

We can thus implement the discrete form of the right hand side of (5.5), analogous to the right hand side of (4.4), by applying suitable relaxation times to the different moments, then reconstructing the post-collisional distributions from the moments using [23]

$$g_{i\beta} = \frac{1}{2}\left(\xi_{i\alpha}\Lambda_{\alpha\beta} + \xi_{i\gamma}\xi_{i\alpha}M_{\gamma\alpha\beta}\right) \text{ for } i \neq 0, \quad g_{0\beta} = B_\beta - M_{\alpha\alpha\beta}. \tag{5.16}$$

6 Decomposition of the Λ tensor

To proceed further we need a more detailed investigation of the electric field tensor $\mathbf{\Lambda}$, recognising that $\mathbf{\Lambda}$ does not remain antisymmetric under the evolution (5.8). We can decompose $\mathbf{\Lambda}$ into antisymmetric, isotropic, and symmetric-traceless parts as

$$\Lambda_{\alpha\beta} = \frac{1}{2}\left(\Lambda_{\alpha\beta} - \Lambda_{\beta\alpha}\right) + \frac{1}{3}\delta_{\alpha\beta}\Lambda_{\gamma\gamma} + \frac{1}{2}\left(\Lambda_{\alpha\beta} + \Lambda_{\beta\alpha} - \frac{2}{3}\delta_{\alpha\beta}\Lambda_{\gamma\gamma}\right). \tag{6.1}$$

This is the most general decomposition of a three-dimensional rank-2 tensor that is irreducible under rotations. We can write this decomposition as

$$\Lambda_{\alpha\beta} = -\epsilon_{\alpha\beta\gamma}E_\gamma + \Psi\delta_{\alpha\beta} + S_{\alpha\beta}, \tag{6.2}$$

by introducing

$$E_\gamma = -\frac{1}{2}\epsilon_{\alpha\beta\gamma}\Lambda_{\alpha\beta}, \quad \Psi = \frac{1}{3}\Lambda_{\gamma\gamma}, \quad S_{\alpha\beta} = \frac{1}{2}\left(\Lambda_{\alpha\beta} + \Lambda_{\beta\alpha} - \frac{2}{3}\delta_{\alpha\beta}\Lambda_{\gamma\gamma}\right). \tag{6.3}$$

The evolution equation (5.3) for $\mathbf{B}$ then becomes

$$\partial_t \mathbf{B} + \nabla\times\mathbf{E} + \nabla\Psi + \nabla\cdot\mathbf{S} = 0. \tag{6.4}$$

This matches the hyperbolic divergence cleaning equation (1.2b) with an extra term $\nabla\cdot\mathbf{S}$. While it appears natural to identify the antisymmetric part of $\mathbf{\Lambda}$ with the electric field $\mathbf{E}$ as in previous work [23, 25], and the trace of $\mathbf{\Lambda}$ with the additional scalar field Ψ in the divergence-cleaning equations, a slightly different relation is needed to absorb the contribution from $\nabla\cdot\mathbf{S}$.

We choose the matrix elements $\mathbf{L}_{ij}$ so that the right-hand side of (5.8) becomes a linear operator L acting on $\mathbf{\Lambda}^{(1)}$ with eigenvalues $1/\tau_E$, $1/\tau_\Psi$ and $1/\tau_S$ for $\mathbf{E}$, Ψ, and $\mathbf{S}$,

$$\partial_t\Lambda_{\alpha\beta} + \partial_\gamma M_{\gamma\alpha\beta} = -[\mathsf{L}\mathbf{\Lambda}]_{\alpha\beta} = -\frac{1}{\tau_E}(-\epsilon_{\alpha\beta\gamma}E_\gamma) - \frac{1}{\tau_\Psi}\Psi\delta_{\alpha\beta} - \frac{1}{\tau_S}S_{\alpha\beta}. \tag{6.5}$$

We now suppose that τ_S is sufficiently small that we can apply the multiple-scales expansion for the symmetric-traceless part of (6.5). As $\Lambda^{(0)}_{\alpha\beta} = u_\alpha B_\beta - u_\beta B_\alpha$ is antisymmetric, while $M^{(0)}_{\alpha\beta\gamma} = \Theta\delta_{\alpha\beta}B_\gamma$, taking the symmetric-traceless part of (5.11) gives

$$S_{\alpha\beta} = -\frac{1}{2}\tau_S\Theta\left(\partial_\alpha B_\beta + \partial_\beta B_\alpha - \frac{2}{3}\delta_{\alpha\beta}\partial_\gamma B_\gamma\right) + O(\tau^2). \tag{6.6}$$

The error term represents contributions of $O(\tau_S^2)$ and $O(\tau_S\tau_M)$ from the next order in the multiple-scales expansion, where $1/\tau_M$ is the eigenvalue of the collision operator for $\mathbf{M}$. Under this approximation, the electric field tensor becomes

$$\Lambda_{\alpha\beta} = -\epsilon_{\alpha\beta\gamma}E_\gamma + \Psi\delta_{\alpha\beta} - \frac{1}{2}\tau_S\Theta\left(\partial_\alpha B_\beta + \partial_\beta B_\alpha - \frac{2}{3}\delta_{\alpha\beta}\partial_\gamma B_\gamma\right) + O(\tau^2). \tag{6.7}$$

Only $\mathbf{S}$ has been expressed in terms of $\mathbf{B}$ and its derivatives using the multiple-scales expansion. We have made no similar assumption for $\mathbf{E}$ or Ψ. The eigenvalue $1/\tau_S$ must be finite for the collision operator to be invertible, so we cannot avoid the contribution from $\nabla\cdot\mathbf{S}$ in (6.4). However, following the approach used to construct the symmetric Maxwell stress tensor from the canonical electromagnetic stress tensor [27, 28], we can add a manifestly divergence-free tensor to $\mathbf{\Lambda}$ to form

$$\widetilde{\Lambda}_{\alpha\beta} = \Lambda_{\alpha\beta} - \tau_S\Theta\partial_\gamma\left(\delta_{\beta\alpha}B_\gamma - \delta_{\beta\gamma}B_\alpha\right). \tag{6.8}$$

The expression in $(\cdots)$ is antisymmetric in the α and γ indices, so $\partial_\alpha\widetilde{\Lambda}_{\alpha\beta} = \partial_\alpha\Lambda_{\alpha\beta}$, while

$$\widetilde{\Lambda}_{\alpha\beta} = -\epsilon_{\alpha\beta\gamma}\left(E_\gamma - \frac{1}{2}\tau_S\Theta\epsilon_{\gamma\mu\nu}\partial_\mu B_\nu\right) + \delta_{\alpha\beta}\left(\Psi - \frac{2}{3}\tau_S\Theta\partial_\gamma B_\gamma\right) + O(\tau^2). \tag{6.9}$$

The equation $\partial_t\mathbf{B} + \nabla\cdot\widetilde{\mathbf{\Lambda}} = 0$ thus becomes

$$\partial_t\mathbf{B} + \nabla\times\left(\mathbf{E} + \frac{1}{2}\tau_S\Theta\nabla\times\mathbf{B}\right) + \nabla\left(\Psi - \frac{2}{3}\tau_S\Theta\nabla\cdot\mathbf{B}\right) = O(\tau^2). \tag{6.10}$$

This now matches the postulated form [6–8, 18]

$$\partial_t\mathbf{B} + \nabla\times\widetilde{\mathbf{E}} + \nabla\widetilde{\Psi} = 0 \tag{6.11}$$

if we define the effective electric and scalar fields

$$\widetilde{\mathbf{E}} = \mathbf{E} + \frac{1}{2}\tau_S\Theta\nabla\times\mathbf{B}, \quad \widetilde{\Psi} = \Psi - \frac{2}{3}\tau_S\Theta\nabla\cdot\mathbf{B}. \tag{6.12}$$

The coefficient of $\tau_S\Theta\nabla\cdot\mathbf{B}$ in the definition of $\widetilde{\Psi}$ is $1/D - 1$ in D spatial dimensions, equal to $-2/3$ as shown in three dimensions, and equal to $-1/2$ in two dimensions.

The existence of the transformation (6.12) to absorb the contribution from $\nabla\cdot\mathbf{S}$ is a consequence of the Helmholtz decomposition theorem, by which the vector field $\partial_t\mathbf{B}$ can always be expressed uniquely as the sum of the curl of a vector field and the gradient of a scalar field [46, 47]. However, these explicit formulae for $\widetilde{\mathbf{E}}$ and $\widetilde{\Psi}$ arise from using the multiple-scales expansion to express $\mathbf{S}$ in terms of the spatial derivatives of $\mathbf{B}$.

As a check that we can recover existing results from this decomposition, applying the multiple-scales expansion for the single relaxation time collision operator $\mathbf{L}_{ij} = (1/\tau_{\mathbf{\Lambda}})\mathbf{I}\delta_{ij}$ gives

$$\mathbf{E} = -\frac{1}{2}\boldsymbol{\epsilon}:\mathbf{\Lambda} = -\mathbf{u}\times\mathbf{B} + \frac{1}{2}\tau_{\mathbf{\Lambda}}\Theta\nabla\times\mathbf{B}, \quad \Psi = \frac{1}{3}\mathrm{Tr}\mathbf{\Lambda} = -\frac{1}{3}\tau_{\mathbf{\Lambda}}\Theta\nabla\cdot\mathbf{B}, \tag{6.13}$$

on neglecting $O({\tau_{\mathbf{\Lambda}}}^2)$ errors. The : denotes a double tensor contraction between the alternating tensor $\boldsymbol{\epsilon}$ and $\mathbf{\Lambda}$. Equations (6.10) and (6.12) then rearrange into

$$\partial_t\mathbf{B} = \nabla\times(\mathbf{u}\times\mathbf{B} - \eta\nabla\times\mathbf{B}) + \nabla(\eta\nabla\cdot\mathbf{B}). \tag{6.14}$$

This is the usual evolution equation for lattice Boltzmann MHD with constant resistivity $\eta = \tau_{\mathbf{\Lambda}}\Theta$ and parabolic divergence cleaning [22, 23, 25].

6.1 Modified telegraph equation

More generally, but still assuming that the relaxation time τ_M is sufficiently short that we may replace $\mathbf{M}$ by $\mathbf{M}^{(0)}$ in (6.5) to sufficient accuracy, the scalar field $\Psi = \frac{1}{3}\mathrm{Tr}\boldsymbol{\Lambda}$ evolves according to

$$\partial_t \Psi + \frac{1}{3}\Theta \nabla\cdot\mathbf{B} = -\frac{1}{\tau_\Psi}\Psi, \tag{6.15}$$

which we can rewrite as

$$\tau_\Psi \partial_t \Psi + \Psi = -\frac{1}{3}\tau_\Psi \Theta \nabla\cdot\mathbf{B}. \tag{6.16}$$

The scalar field $\widetilde{\Psi} = \Psi - \frac{2}{3}\tau_S \Theta \nabla\cdot\mathbf{B}$ defined in (6.12) then evolves according to

$$\tau_\Psi \partial_t \widetilde{\Psi} + \widetilde{\Psi} = -\frac{1}{3}\Theta\left((\tau_\Psi + 2\tau_S)\nabla\cdot\mathbf{B} + 2\tau_S\tau_\Psi \partial_t \nabla\cdot\mathbf{B}\right). \tag{6.17}$$

Eliminating $\nabla\cdot\mathbf{B}$ using $\partial_t \nabla\cdot\mathbf{B} + \nabla^2\widetilde{\Psi} = 0$ gives the modified telegraph equation

$$\tau_\Psi \partial_{tt}\widetilde{\Psi} + \left(1 - \frac{2}{3}\Theta\tau_S\tau_\Psi\nabla^2\right)\partial_t\widetilde{\Psi} = \frac{1}{3}\Theta(\tau_\Psi + 2\tau_S)\nabla^2\widetilde{\Psi}. \tag{6.18}$$

This equation is also satisfied by $\nabla\cdot\mathbf{B}$. It resembles the earlier telegraph equation (1.3) with an extra term $\nabla^2\partial_t\widetilde{\Psi}$ due to the symmetric part of the electric field tensor $\boldsymbol{\Lambda}$. This extra term can be made small by choosing $\tau_S \ll \tau_\Psi$, but we need $\tau_S > 0$ for invertibility of the collision operator.

Solutions of (6.18) proportional to $\exp(i\mathbf{k}\cdot\mathbf{x} - \lambda t)$ exist when λ satisfies the dispersion relation

$$\lambda = \frac{1}{6\tau_\Psi}\left[3 + 2\epsilon\Theta k^2\tau_\Psi^2 \pm \left((3 + 2\epsilon\Theta k^2\tau_\Psi^2)^2 - 12\Theta k^2\tau_\Psi^2(1+2\epsilon)\right)^{1/2}\right], \tag{6.19}$$

where $\epsilon = \tau_S/\tau_\Psi$ and $k = |\mathbf{k}|$. This dispersion relation has wave-like oscillatory solutions with λ complex when the wavenumber k lies in the range $k_- < k < k_+$ with

$$k_\pm = \sqrt{\frac{6}{\Theta}}\frac{1}{2\epsilon\tau_\Psi}\left(1 + \epsilon \pm \sqrt{1+2\epsilon}\right)^{1/2}. \tag{6.20}$$

The function $K(\epsilon) = (1+\epsilon-\sqrt{1+2\epsilon})/\epsilon^2$ is a non-negative, monotonic decreasing function of ϵ with $K(\epsilon) \to 1/2$ as $\epsilon \to 0$. The range of wavenumbers for which oscillatory solutions exist in (6.18) then approaches the range $k > \sqrt{3/\Theta}/(2\tau_\Psi)$ for which oscillatory solutions exist in the telegraph equation with $\tau_S = 0$.

6.2 Viscoelastic fluid analogy

A transformation similar to that from $\mathbf{E}$ and Ψ to $\widetilde{\mathbf{E}}$ and $\widetilde{\Psi}$ in (6.12) arises in models for viscoelastic fluids. The linear Maxwell model describes the elastic stress $\boldsymbol{\sigma}_p$ due to polymer molecules suspended in a Newtonian viscous fluid using

$$\tau \partial_t \boldsymbol{\sigma}_p + \boldsymbol{\sigma}_p = \mu' \mathbf{e}, \tag{6.21}$$

where $\mathbf{e} = \nabla \mathbf{u} + (\nabla \mathbf{u})^{\mathsf{T}}$ is the strain rate. The parameters are the stress relaxation time τ and the steady-state viscosity μ'. The total deviatoric stress is $\boldsymbol{\sigma} = \mu \mathbf{e} + \boldsymbol{\sigma}_p$ with a further Newtonian viscous stress $\mu \mathbf{e}$ from the suspending fluid. The total deviatoric stress thus evolves according to the Jeffreys model [48, 49]

$$\tau \partial_t \boldsymbol{\sigma} + \boldsymbol{\sigma} = (\mu + \mu') \left(\mathbf{e} + \frac{\mu}{\mu + \mu'} \tau \partial_t \mathbf{e} \right). \tag{6.22}$$

This becomes the Oldroyd–B viscoelastic model if we replace the partial time derivatives with upper convected derivatives [49, 50].

If we suppose that the fluid velocity is a shear flow of the form $\mathbf{u} = w(x,y,t)\mathbf{e}_z$, so that $\mathbf{u} \cdot \nabla \mathbf{u} = 0$, the momentum equation becomes $\rho_0 \partial_t \mathbf{u} = \nabla \cdot \boldsymbol{\sigma}$ for a fluid with constant density ρ_0. There is no contribution from the pressure. The divergence of $\boldsymbol{\sigma}$ satisfies

$$\tau \partial_t \nabla \cdot \boldsymbol{\sigma} + \nabla \cdot \boldsymbol{\sigma} = (\mu + \mu') \left(\nabla^2 \mathbf{u} + \frac{\mu}{\mu + \mu'} \tau \partial_t \nabla^2 \mathbf{u} \right), \tag{6.23}$$

so the velocity $\mathbf{u}$ satisfies the same modified telegraph equation as $\widetilde{\Psi}$,

$$\tau \partial_{tt} \mathbf{u} + \left(1 - \nu \tau \nabla^2\right) \partial_t \mathbf{u} = (\nu + \nu') \nabla^2 \mathbf{u}. \tag{6.24}$$

The parameters $\nu' = \mu'/\rho_0$ and $\nu = \mu/\rho_0$ are the kinematic viscosities associated with the polymer molecules and the suspending fluid respectively. The two equations coincide exactly if we take $\tau = \tau_\Psi$, $\nu = (2/3)\Theta\tau_S$ and $\nu' = (1/3)\Theta\tau_\Psi$.

7 Implementation

To implement hyperbolic divergence cleaning with an adjustable parameter, we simply adjust the matrices $\mathbf{L}_{ij}$ to apply a different relaxation time τ_Ψ to $\Psi = \frac{1}{3}\mathrm{Tr}\boldsymbol{\Lambda}$ in the decomposition (6.3). The collision operator in the discrete scheme acts on transformed tensors computed from transformed vector distribution functions:

$$\overline{\boldsymbol{\Lambda}} = \sum_{i=0}^{M} \boldsymbol{\xi}_i \overline{\mathbf{g}}_i, \quad \overline{\mathbf{M}} = \sum_{i=0}^{M} \boldsymbol{\xi}_i \boldsymbol{\xi}_i \overline{\mathbf{g}}_i, \quad \overline{\mathbf{g}}_i = \mathbf{g}_i + \frac{1}{2}\Delta t \sum_{j=0}^{M} \mathbf{L}_{ij} \left(\mathbf{g}_j - \mathbf{g}_j^{(0)} \right). \tag{7.1}$$

This change of variables, analogous to that from f_i to $\overline{f}_i$ in Section 4, gives a discrete scheme with second-order accuracy.

A minimal discrete collision operator with the required property in three dimensions computes the post-collisional electric field tensor $\overline{\mathbf{\Lambda}}'$ as

$$\overline{\mathbf{\Lambda}}' = \mathbf{\Lambda}^{(0)} + \frac{\tau_{\mathbf{\Lambda}} - \Delta t/2}{\tau_{\mathbf{\Lambda}} + \Delta t/2}\left(\overline{\mathbf{\Lambda}} - \mathbf{\Lambda}^{(0)}\right) + \frac{1}{3}\mathbf{I}\left(\frac{\tau_{\Psi} - \Delta t/2}{\tau_{\Psi} + \Delta t/2} - \frac{\tau_{\mathbf{\Lambda}} - \Delta t/2}{\tau_{\mathbf{\Lambda}} + \Delta t/2}\right)\mathrm{Tr}\,\overline{\mathbf{\Lambda}}. \tag{7.2}$$

The last term changes the relaxation time applied to $\mathrm{Tr}\,\overline{\mathbf{\Lambda}}$ from $\tau_{\mathbf{\Lambda}}$ to τ_{Ψ}, while having no effect on the traceless part of $\overline{\mathbf{\Lambda}}$. The combinations $\tau_{\Psi} \pm \Delta t/2$ and $\tau_{\mathbf{\Lambda}} \pm \Delta t/2$ arise from the change of variables from $\mathbf{g}_i$ to $\overline{\mathbf{g}}_i$.

Similarly, the post-collisional tensor $\overline{\mathbf{M}}'$ is given by

$$\overline{\mathbf{M}}' = \mathbf{M}^{(0)} + \frac{\tau_M - \Delta t/2}{\tau_M + \Delta t/2}\left(\overline{\mathbf{M}} - \mathbf{M}^{(0)}\right), \tag{7.3}$$

while $\mathbf{B}$ is unaffected by both collisions and the change of variables. We can now reconstruct the post-collisional distribution functions using

$$\overline{g}'_{i\beta} = \tfrac{1}{2}\left(\xi_{i\alpha}\overline{\Lambda}'_{\alpha\beta} + \xi_{i\gamma}\xi_{i\alpha}\overline{M}'_{\gamma\alpha\beta}\right) \text{ for } i \neq 0, \quad \overline{g}'_{0\beta} = B_\beta - \overline{M}'_{\alpha\alpha\beta}, \tag{7.4}$$

and stream them to adjacent lattice points:

$$\overline{\mathbf{g}}_i(\mathbf{x}, t + \Delta t) = \overline{\mathbf{g}}'_i(\mathbf{x} - \boldsymbol{\xi}_i \Delta t, t). \tag{7.5}$$

8 Numerical experiments

Most previous tests of the lattice Boltzmann MHD algorithms and its variants used smooth initial magnetic fields, such as the Orszag–Tang vortex and the doubly-periodic coalescence instability [22]. These smooth fields can be accurately represented on a finite lattice, so any discrete analog of $\nabla \cdot \mathbf{B}$ will be extremely small. The divergence cleaning equations exactly coincide with Maxwell's equations when $\nabla \cdot \mathbf{B} = 0$.

To see the consequence of a nonzero discrete analog of $\nabla \cdot \mathbf{B}$, we adopt a smoothed version of DeVore's [11] benchmark for a two-dimensional current-carrying cylinder. Any magnetic field of the form

$$B_x = -y f(r), \quad B_y = x f(r), \quad r = \sqrt{x^2 + y^2}, \tag{8.1}$$

satisfies $\nabla \cdot \mathbf{B} = 0$ analytically, but any discrete analog of $\nabla \cdot \mathbf{B}$ will be nonzero due to truncation error. We use a smoothed tanh profile in r,

$$f(r) = \frac{1}{2r_{\max}}\left(1 + \tanh\left(\frac{r_{\max} - r}{\delta r}\right)\right), \tag{8.2}$$

instead of the step function used by DeVore [11]. The lattice Boltzmann algorithm presented here solves the viscous and resistive MHD equations. It does not include flux or

slope limiters to accommodate the discontinuous solutions that are permitted by the ideal MHD equations. The factor of $1/r_{\max}$ in the definition of $f(r)$ ensures that $\max|\mathbf{B}| \approx 1$, which is convenient for scaling purposes.

If we suppose that the magnetic field is sufficiently weak, so that the Lorentz force is negligible, we can derive a closed pair of evolution equations for $\Psi = \frac{1}{2}\mathrm{Tr}\boldsymbol{\Lambda}$ and $\delta = \nabla\cdot\mathbf{B}$,

$$\partial_t \Psi + \frac{1}{2}\Theta\delta = -\frac{1}{\tau_\Psi}\Psi, \quad \partial_t \delta = \nabla^2\left(\frac{1}{2}\tau_S\Theta\delta - \Psi\right). \tag{8.3}$$

We formulate an evolution equation for Ψ, rather than $\widetilde{\Psi} = \Psi - \frac{1}{2}\tau_S\Theta\nabla\cdot\mathbf{B}$, because Ψ can be directly computed from the magnetic distribution functions in the discrete scheme. Having promoted $\mathrm{Tr}\boldsymbol{\Lambda}$ to be a freely evolving variable, we can no longer use a Chapman–Enskog expansion to approximate $\nabla\cdot\mathbf{B}$ using $\mathrm{Tr}\boldsymbol{\Lambda}$ as in (5.12).

We turn the weak magnetic field approximation into an exact linearisation by omitting the Maxwell stress from $\boldsymbol{\Pi}^{(0)}$ and the $f_i^{(0)}$. The qualitative behaviour is the same as in simulations of the full system with a weak initial magnetic field. We use a two-dimensional domain $[-50,50]^2$ with periodic boundary conditions, and parameters $r_{\max}=8$ and $\delta r = 1$ in the initial conditions. We take the Mach number to be $\sqrt{3}/156$, and the fluid and magnetic Reynolds numbers to be 100. This determines the single relaxation time that we use for the hydrodynamic variables, and the relaxation time τ_E for the anti-symmetric part of $\boldsymbol{\Lambda}$, to be around 10^{-6} in the dimensionless variables we use to formulate the system of partial differential equations. We set the relaxation rate τ_S equal to the relaxation rate τ_E, and set $\tau_M = 10^{-4}\tau_E$ so that $\mathbf{M}$ remains very close to equilibrium.

We initialise the distribution functions for a fluid at rest ($\mathbf{u} = 0$) with this magnetic field using the consistent initialisation algorithm described in the appendix. This creates a small but non-zero initial value for $\Psi = \frac{1}{2}\mathrm{Tr}\boldsymbol{\Lambda}$. Inverting the transformation (7.1) from $\mathbf{g}_i$ to $\overline{\mathbf{g}}_i$ gives Ψ in terms of the $\overline{\mathbf{g}}_i$ in the numerical algorithm,

$$\Psi = \frac{1}{2}\mathrm{Tr}\boldsymbol{\Lambda} = \frac{1}{2}\frac{\tau_\Psi}{\tau_\Psi + \Delta t/2}\mathrm{Tr}\overline{\boldsymbol{\Lambda}}. \tag{8.4}$$

We approximate $\nabla\cdot\mathbf{B}$ using the finite difference formula

$$\Delta = \frac{1}{2}(1+4\tau_S\tau_M)\Delta^+ + \frac{1}{2}(1-4\tau_S\tau_M)\Delta^\times. \tag{8.5}$$

This is a convex linear combination of the two natural finite difference approximations

$$\Delta^+(\mathbf{x},t) = \frac{1}{2\Delta x}\sum_{|\boldsymbol{\xi}_i|=1}\boldsymbol{\xi}_i\cdot\mathbf{B}(\mathbf{x}+\boldsymbol{\xi}_i\Delta t,t), \quad \Delta^\times(\mathbf{x},t) = \frac{1}{4\Delta x}\sum_{|\boldsymbol{\xi}_i|=\sqrt{2}}\boldsymbol{\xi}_i\cdot\mathbf{B}(\mathbf{x}+\boldsymbol{\xi}_i\Delta t,t), \tag{8.6}$$

using the four neighbouring points on the axes for Δ^+, and on the diagonals for $\Delta^\times$, as illustrated in Fig. 2. One can show, by considering the discrete evolution of Λ_{xx} and Λ_{yy}, that Δ is the optimal combination of Δ^+ and $\Delta^\times$ for a magnetic collision operator with

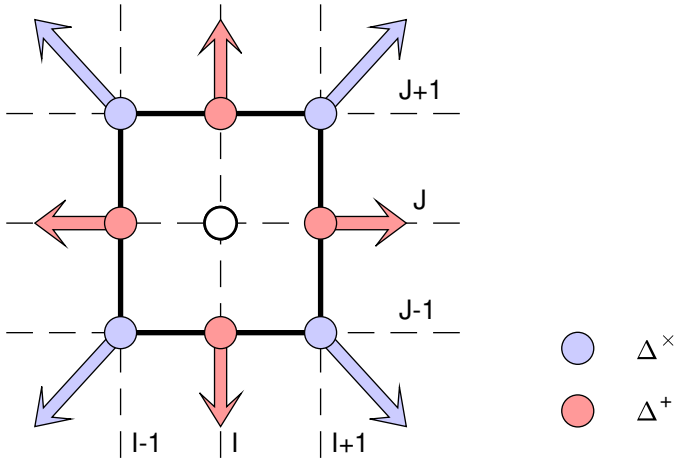

Figure 2: The four points on the coordinate axes used to form Δ^+, and the four points on the corners (longer arrows) used to form $\Delta^\times$. The finite difference formulae Δ^+ and $\Delta^\times$ are both second-order accurate approximations to $\nabla\cdot\mathbf{B}$ at the central point (I,J) marked by an open circle. They both approximate the flux of $\mathbf{B}$ out of the square shown with thick lines.

relaxation times τ_M for $\mathbf{M}$, and τ_S for the symmetric-traceless part of $\mathbf{\Lambda}$. The optimal combination is independent of the relaxation time τ_Ψ for $\mathrm{Tr}\mathbf{\Lambda}$.

The simulations were run on an NVIDIA V100 graphical processor unit using CUDA Fortran. The largest simulation using a 4096×4096 lattice to evolve both the fluid and magnetic variables ran at a speed of 2970 million lattice updates per second (MLUPS). This corresponds to a useful memory bandwidth of 840GB/sec, not far below the theoretical maximum of 900GB/sec. The initialisation procedure described in the appendix was run on the host processor and parallelised using OpenMP. The linear systems were solved using the LAPACK routine ZGESV [51].

Following [24] we can compute reference solutions for the system (8.3) in a domain with periodic boundary conditions using discrete Fourier transforms. For each wavevector $\mathbf{k}$ with modulus k we have a 2×2 matrix system for the Fourier coefficients $\widehat{\Psi}$ and $\widehat{\delta}$,

$$\partial_t\begin{pmatrix}\widehat{\Psi}\\ \widehat{\delta}\end{pmatrix}=\mathsf{A}\begin{pmatrix}\widehat{\Psi}\\ \widehat{\delta}\end{pmatrix}\quad\text{with}\quad\mathsf{A}=\begin{pmatrix}-1/\tau_\Psi & \Theta/2\\ k^2 & -\tau_S\Theta k^2/2\end{pmatrix}. \tag{8.7}$$

The solution of the initial value problem can be written as

$$\begin{pmatrix}\widehat{\Psi}(t)\\ \widehat{\delta}(t)\end{pmatrix}=\exp(t\mathsf{A})\begin{pmatrix}\widehat{\Psi}(0)\\ \widehat{\delta}(0)\end{pmatrix} \tag{8.8}$$

using the matrix exponential

$$\exp(t\mathsf{A})=\exp(-\beta t)\left\{\cosh(\alpha t)\begin{pmatrix}1&0\\0&1\end{pmatrix}+\frac{1}{\alpha}\sinh(\alpha t)\begin{pmatrix}\beta&\Theta/2\\k^2&-\beta\end{pmatrix}\right\} \tag{8.9}$$

with coefficients

$$\alpha = \frac{1}{\tau_\Psi}\left(1+k^2\Theta(2\tau_\Psi-\tau_S)\tau_\Psi+k^4\Theta^2\tau_S^2\tau_\Psi^2/4\right)^{1/2}, \quad \beta = k^2\tau_S\Theta/4+1/(2\tau_\Psi). \tag{8.10}$$

This gives an analytical solution for the Fourier coefficients $\widehat{\Psi}$ and $\widehat{\delta}$, and hence a semi-analytical solution of (8.3) given the discrete Fourier transform of the initial conditions. We used the initial $\Psi = \frac{1}{2}\mathrm{Tr}\boldsymbol{\Lambda}$ and $\Delta \approx \nabla\cdot\mathbf{B}$ computed from the initialised distribution functions $\overline{\mathbf{g}}_i$, and the fast Fourier transform library FFTW3 [52].

Figure 3 shows these initial conditions for a numerical experiment with $\tau_\Psi = 0.01$ using a 4096×4096 lattice. Figure 3 also shows the initial current computed from $\Lambda_{xy}-\Lambda_{yx}$, and the convergence of the initial Ψ and Δ towards zero with increasing spatial resolution.

Figures 4 and 5 show the evolution of Ψ and Δ for two different numerical experiments with $\tau_\Psi = 0.01$ and $\tau_\Psi = 0.1$, both computed on a 4096×4096 lattice. Both values of τ_Ψ are much larger than the relaxation time $\tau_E \approx 10^{-6}$ that determines the resistivity, but the solution with $\tau_\Psi = 0.01$ still shows diffusive behaviour. The supports of both Ψ and Δ, the regions of space over which these fields are non-zero, are well approximated by circular discs that expand with time. The two fields also have very similar spatial structures. This is consistent with $\Psi = -\frac{1}{2}\tau_\Psi\Theta\nabla\cdot\mathbf{B}+O(\tau_\Psi^2)$ from the Chapman–Enskog solution that is valid when τ_Ψ is sufficiently small. By contrast, the second solution with $\tau_\Psi = 0.1$ shown in Fig. 5 show a hyperbolic behaviour. The support of Δ is confined to two concentric expanding annuli, each quite narrow, while the support of Ψ also includes the region between these two annuli. The supports have expanded more quickly than those shown in Fig. 4, and the spatial structures of Ψ and Δ are noticably different.

Figures 6 and 7 show the ℓ^2-norms of the relative errors in Ψ and Δ computed using the Fourier-based reference solution for the same initial conditions. The relative errors are quite large in all cases, because the initial fields, and hence the amplitude of the reference solution are small, and become smaller as the spatial resolution increases (see Fig. 3(d)). The Ψ field appears to be computed with second-order accuracy, while Δ is only a first-order accurate approximation to $\nabla\cdot\mathbf{B}$ in the reference solution. This may be because the finite difference approximation (8.5) is not completely consistent with the discrete evolution of $\mathbf{B}$ under the lattice Boltzmann algorithm with separately evolving $\boldsymbol{\Lambda}$ and $\mathbf{M}$ fields. However, Fig. 8 show that the computed solutions remain visually indistinguishable from the reference solutions, even at later times when the effects of the periodic boundary conditions are clearly visible.

9 Conclusions

Numerical algorithms for simulating magnetohydrodynamics typically do not preserve $\nabla\cdot\mathbf{B} = 0$, and so are inconsistent with Maxwell's equations. This can lead to artifacts in the computed solutions, because structural properties of the MHD equations cease to hold [1–4]. There have been several approaches to improve the structural properties of

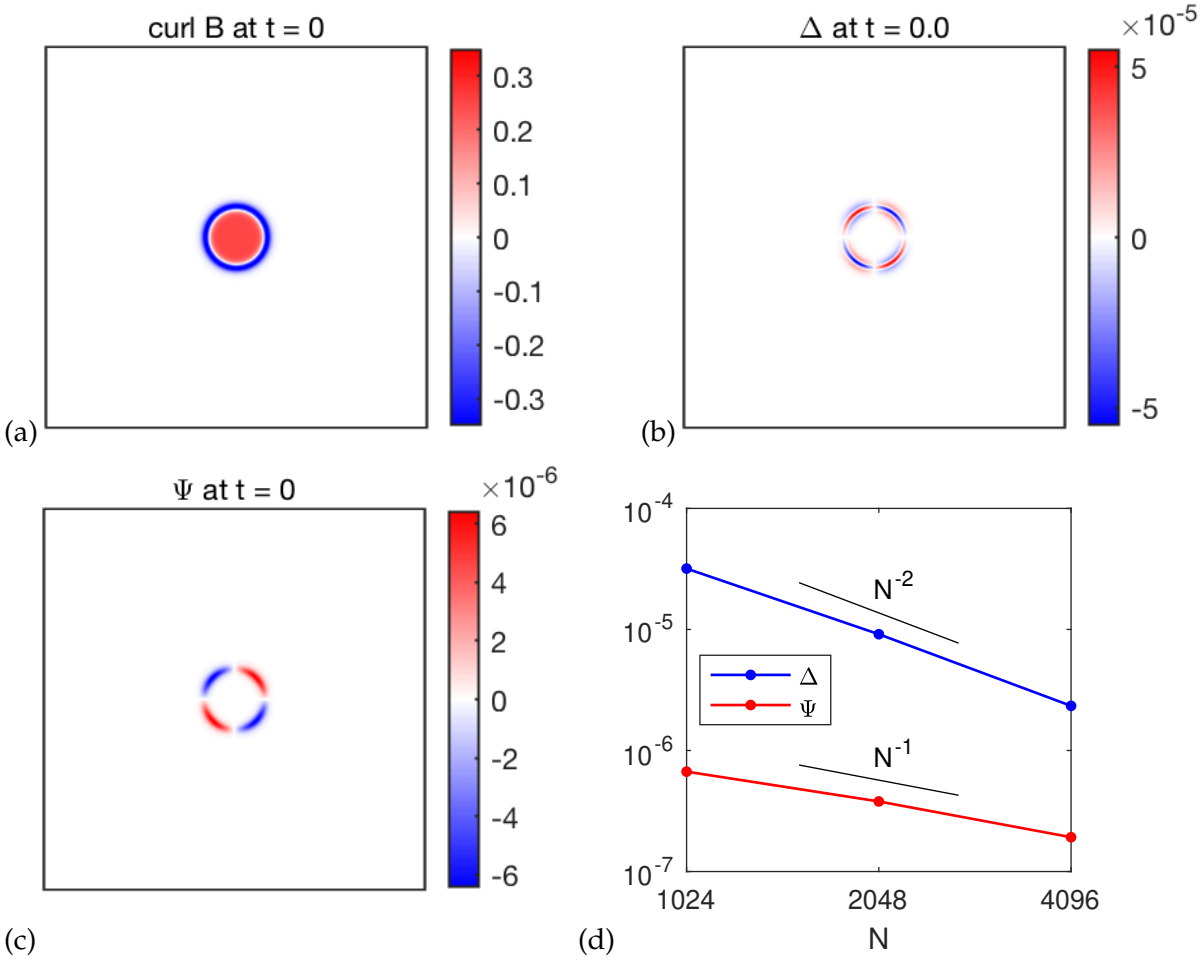

Figure 3: The initial fields from the consistent initialisation, (a) current $\hat{\mathbf{z}}\cdot\nabla\times\mathbf{B}$, (b) discrete divergence $\Delta\approx\nabla\cdot\mathbf{B}$, and (c) scalar field Ψ, computed on a $N\times N$ lattice with $\tau_\Psi=0.01$ and $N=4096$. Panel (d) shows the different rates of convergence of the ℓ^2-norms of Δ and Ψ towards zero with increasing N. Convergence appears to be second order for $\nabla\cdot\mathbf{B}$, but only first order for Ψ.

the equation set being solved by including extra terms proportional to $\nabla\cdot\mathbf{B}$. This can be motivated by considering an extended set of Maxwell equations that includes magnetic charges and magnetic currents. Powell [32,33] proposed that $\nabla\cdot\mathbf{B}$ should advect with the fluid velocity $\mathbf{u}$, while Dedner *et al.* [18] proposed that $\nabla\cdot\mathbf{B}$ should propagate and decay isotropically according to a telegraph equation.

The original lattice Boltzmann MHD algorithm already solves an extended set of Maxwell equations, since it replaces $\partial_t\mathbf{B}+\nabla\times\mathbf{E}=0$ with $\partial_t\mathbf{B}+\nabla\cdot\mathbf{\Lambda}=0$. The two equations are equivalent when $\Lambda_{\alpha\beta}=-\epsilon_{\alpha\beta\gamma}E_\gamma$ is purely antisymmetric. However, $\mathbf{\Lambda}$ is itself an evolving variable in our kinetic formulation. The tensor $\mathbf{\Lambda}$ develops a symmetric part, even though its equilibrium form $\mathbf{\Lambda}^{(0)}$ is purely antisymmetric. The symmetric part of

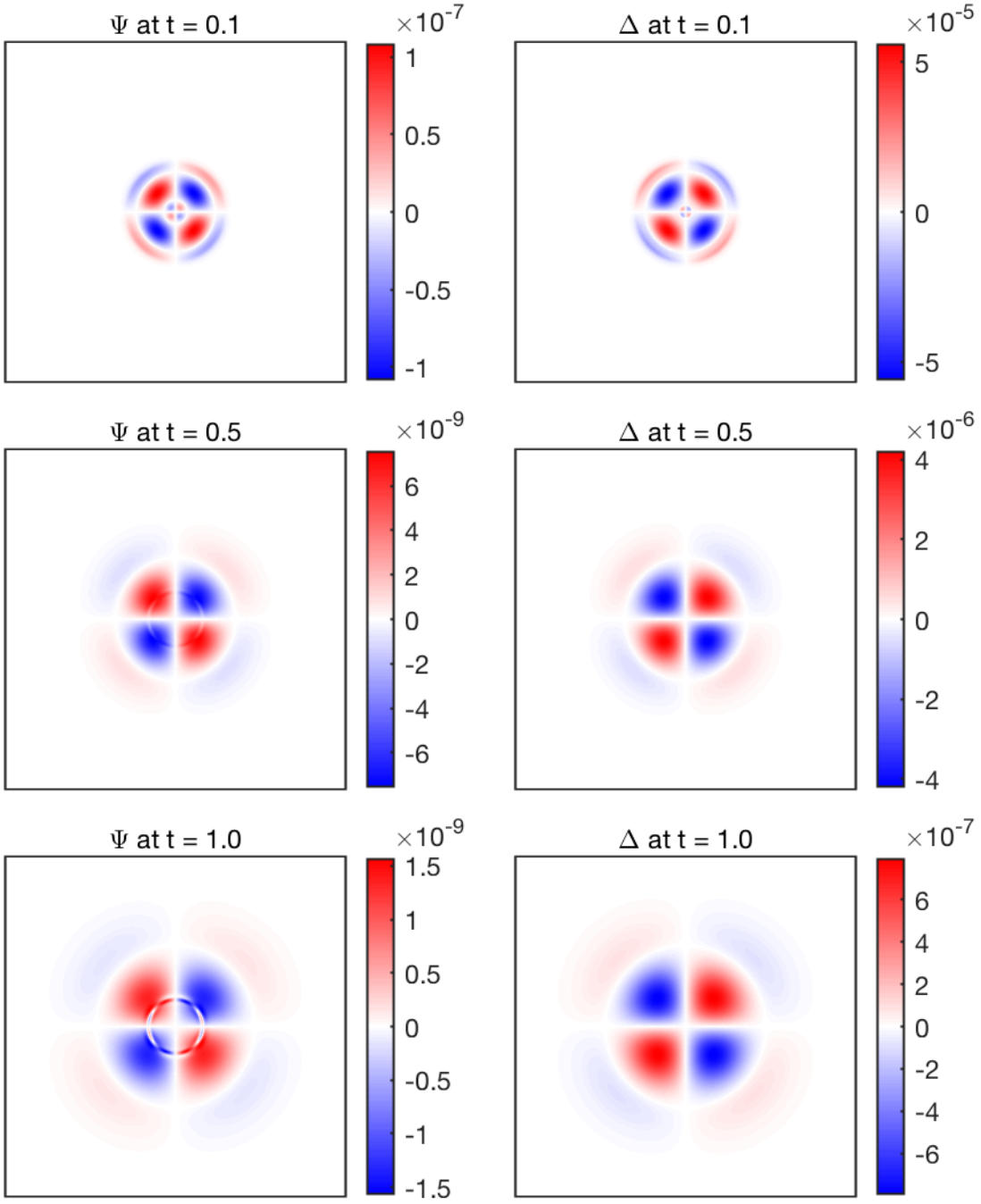

Figure 4: Evolution of Ψ and Δ over time for $\tau_\Psi = 0.01$. The fields Ψ and $-\Delta$ have very similar spatial structures, consistent with $\Psi = -\frac{1}{2}\tau_\Psi \Theta \nabla \cdot \mathbf{B} + O(\tau_\Psi^2)$ in the Chapman–Enskog solution..

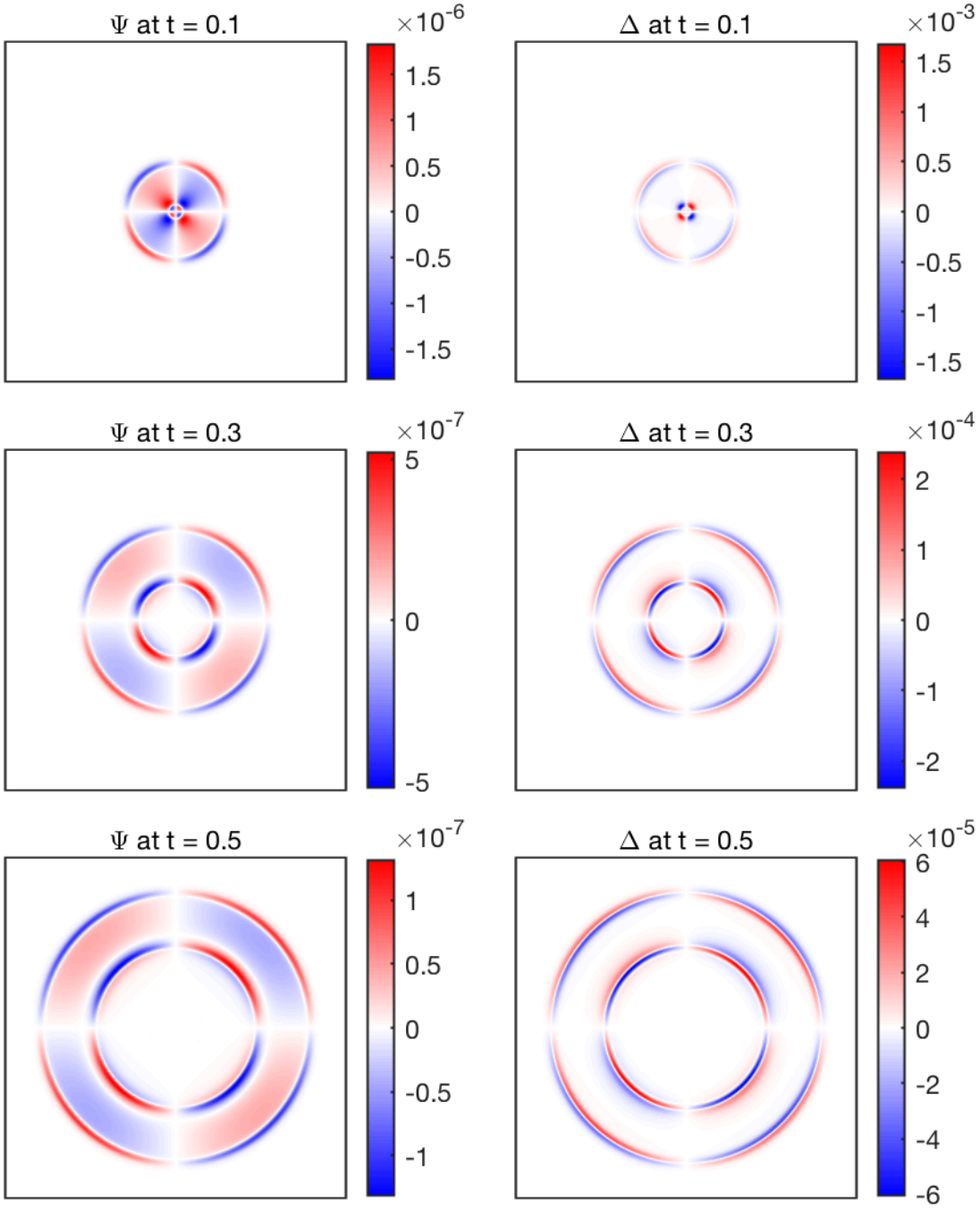

Figure 5: Evolution of Ψ and Δ over time for $\tau_\Psi = 0.1$. The two fields have distinctly different spatial structures for this larger value of τ_Ψ. In particular, Ψ is non-zero in the annulus bounded by the two concentric annuli on which Δ is non-zero.

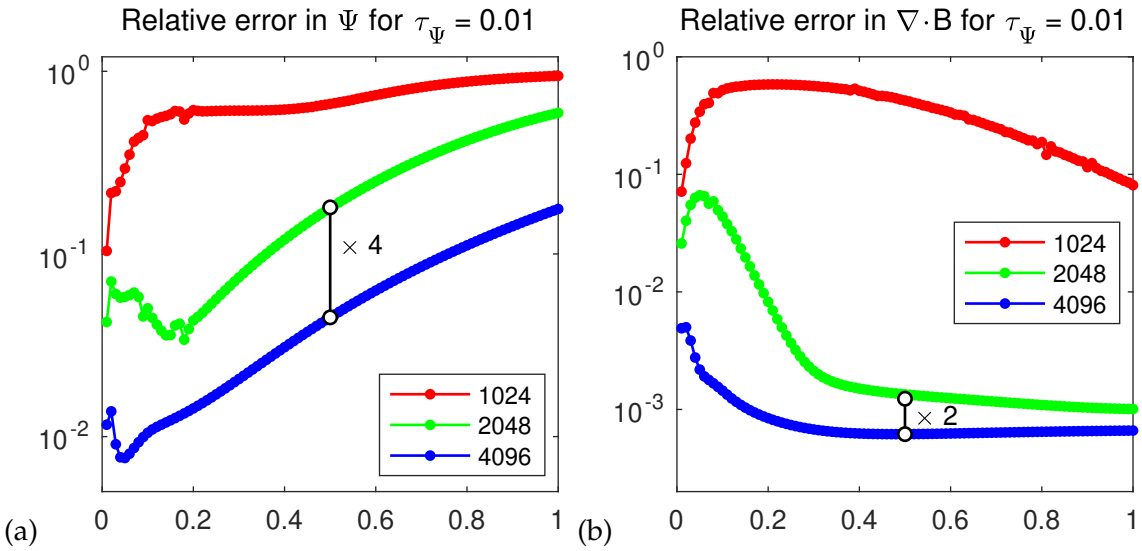

Figure 6: Relative errors in (a) Ψ, and (b) Δ approximating $\nabla\cdot\mathbf{B}$, versus the reference solutions with $\tau_\Psi = 0.01$ for $N\times N$ lattices with $N = 1024$, 2048, 4096.

$\mathbf{\Lambda}$ provides the parabolic divergence cleaning term $\nabla(\eta\nabla\cdot\mathbf{B})$ in the induction equation (1.6) simulated by the first version of the lattice Boltzmann MHD algorithm [22] when one computes the first correction $\mathbf{\Lambda}^{(1)}$ to $\mathbf{\Lambda}^{(0)}$ via a Chapman–Enskog expansion.

However, the underlying kinetic equation (5.5) is a hyperbolic system for the magnetic distribution functions $\mathbf{g}_i$, or equivalently for the basis of moments $\mathbf{B}$, $\mathbf{\Lambda}$, $\mathbf{M}$. Parabolic behaviour, as in resistive MHD, only emerges from employing a Chapman–Enskog expansion to find slowly varying solutions for the variables that are conserved, or vary slowly, under collisions. By modifying the collision operator applied to the $\mathbf{g}_i$ we can impose a different and much longer relaxation time τ_Ψ for the trace of the $\mathbf{\Lambda}$ tensor, while the remaining antisymmetric and symmetric-traceless parts relax with much shorter relaxation times τ_E and τ_S respectively. We can then recover the hyperbolic divergence-cleaning system studied by Dedner *et al.* [18] by identifying their scalar field Ψ with $\mathrm{Tr}\mathbf{\Lambda}$, up to a small modification proportional to the relaxation time τ_S applied to the symmetric-traceless part of $\mathbf{\Lambda}$. This modification can be made small by taking τ_S small, but we need $\tau_S > 0$ for the collision matrix to be invertible. The resulting modified telegraph equation satisfied by Ψ and $\nabla\cdot\mathbf{B}$ coincides with the equation satisfied by the velocity field for shear flows using the linear Jeffreys model for viscoelastic fluids [48, 49].

Acknowledgement

The computations employed the Advanced Research Computing facilities at the University of Oxford [53].

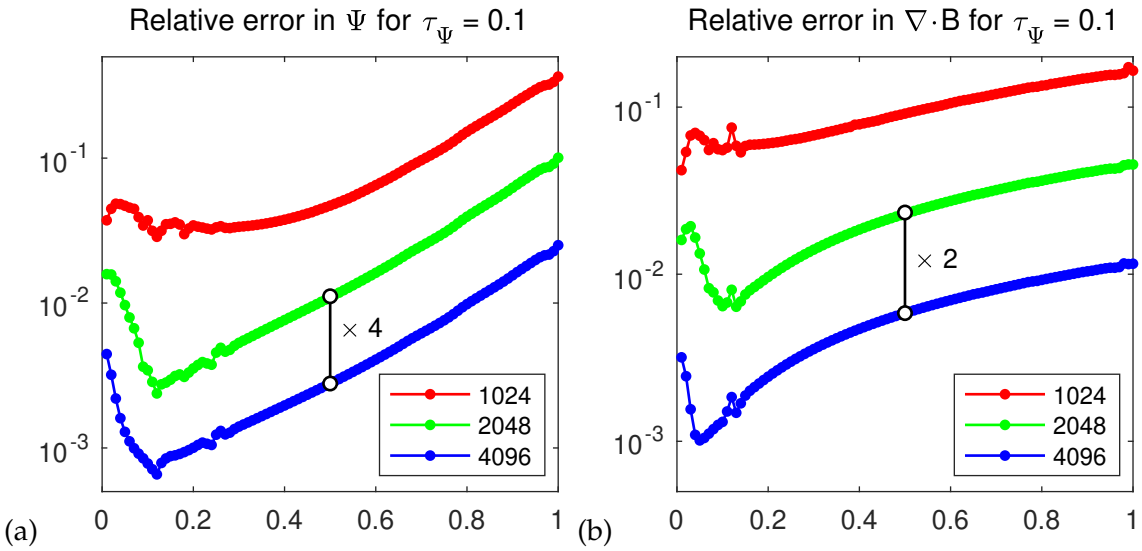

Figure 7: Relative errors in (a) Ψ, and (b) Δ approximating $\nabla\cdot\mathbf{B}$, versus the reference solutions with $\tau_\Psi = 0.1$ for $N\times N$ lattices with $N = 1024$, 2048, 4096.

A Consistent initialisation

For accurate results, the non-equilibrium part of the distributions functions must be initialised consistently with the equilibrium. For example, the non-equilibrium part of $\mathbf{\Lambda}$ must depend upon the spatial derivatives of the initial magnetic field to match the Chapman–Enskog solution from Section 5. We do this by seeking a steady solution, one that solves

$$f_i(\mathbf{x}+\boldsymbol{\xi}_i\Delta t) = f_i(\mathbf{x}) - \frac{\Delta t}{\tau+\Delta t/2}\left(f_i(\mathbf{x}) - f_i^{(0)}(\mathbf{x})\right), \tag{A.1}$$

and

$$\mathbf{g}_i(\mathbf{x}+\boldsymbol{\xi}_i\Delta t) = \mathbf{g}_i(\mathbf{x}) + \mathsf{L}_{ij}\left(\mathbf{g}_j(\mathbf{x}) - \mathbf{g}_j^{(0)}(\mathbf{x})\right), \tag{A.2}$$

where $f_i^{(0)}(\mathbf{x})$ and $\mathbf{g}_j^{(0)}(\mathbf{x})$ are known functions of the prescribed initial ρ, $\mathbf{u}$ and $\mathbf{B}$. This is equivalent to assuming that the non-equilibrium part will approach the Chapman–Enskog solution on a timescale much shorter than the timescale on which the macroscopic variables ρ, $\mathbf{u}$ and $\mathbf{B}$ evolve. We have used a simple single-relaxation-time collision operator for the hydrodynamic distribution functions in (A.1) for simplicity.

Taking a discrete Fourier transform of (A.1) gives, for each wavevector $\mathbf{k}$,

$$\left(\exp(i\Delta t\mathbf{k}\cdot\boldsymbol{\xi}_i) - 1\right)\widehat{f}_i = -\frac{\Delta t}{\tau+\Delta t/2}\left(\widehat{f}_i - \widehat{f}_i^{(0)}\right), \tag{A.3}$$

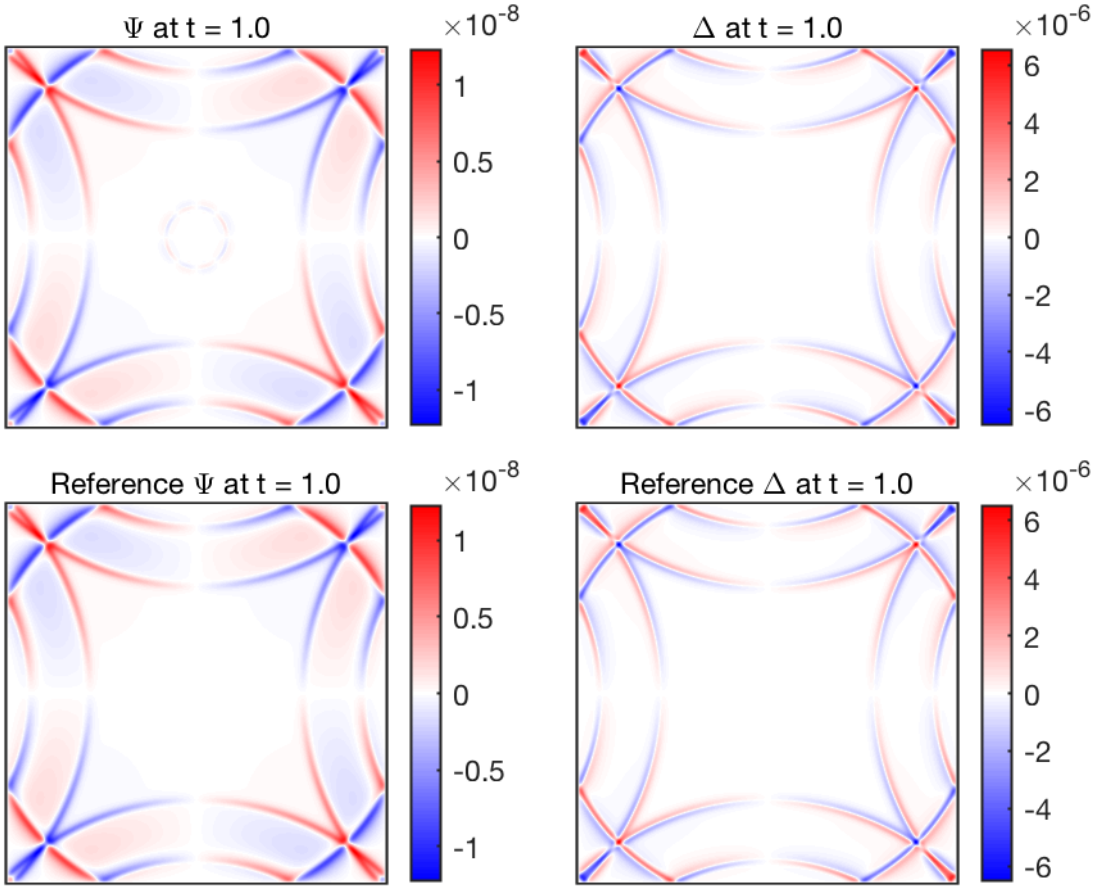

Figure 8: The computed fields Ψ and Δ are visually indistinguishable from the reference solutions, even at later times when the effects of the periodic boundary conditions are clearly visible.

where $\widehat{f}_i$ and $\widehat{f}_i^{(0)}$ are the discrete Fourier transforms of f_i and $f_i^{(0)}$. We can now solve for

$$\widehat{f}_i = \frac{\Delta t}{\exp(i\Delta t \mathbf{k}\cdot\boldsymbol{\xi}_i)(\tau+\Delta t/2)-(\tau-\Delta t/2)}\widehat{f}_i^{(0)}. \tag{A.4}$$

Similarly, taking a discrete Fourier transform of (A.2) gives, for each wavevector $\mathbf{k}$,

$$\left(\exp(i\Delta t\mathbf{k}\cdot\boldsymbol{\xi}_i)-1\right)\widehat{\mathbf{g}}_i = \mathsf{L}_{ij}\left(\widehat{\mathbf{g}}_j-\widehat{\mathbf{g}}_j^{(0)}\right), \tag{A.5}$$

where $\widehat{\mathbf{g}}_i$ is the discrete Fourier transform of $\mathbf{g}_i$. We now have a general constant collision matrix L_{ij} on the right-hand side. For each $\mathbf{k}$, writing all the $\widehat{\mathbf{g}}_i$ for the different discrete velocities as one vector $\widehat{\mathbf{G}}$ gives

$$\mathsf{D}\widehat{\mathbf{G}} = \mathsf{L}\left(\widehat{\mathbf{G}}-\widehat{\mathbf{G}}^{(0)}\right), \tag{A.6}$$

with all the L_{ij} combined into one matrix L. The left-hand side involves the diagonal matrix

$$\mathsf{D} = \mathrm{diag}\{(\exp(i\Delta t \mathbf{k}\cdot\boldsymbol{\xi}_i) - 1)\,\mathbf{I}\}, \tag{A.7}$$

where $\mathbf{I}$ is the 2×2 identity matrix in two spatial dimensions. We can now solve for

$$\widehat{\mathbf{G}} = (\mathsf{L}-\mathsf{D})^{-1}\mathsf{L}\widehat{\mathbf{G}}^{(0)}. \tag{A.8}$$

This requires the solution of a separate 10×10 linear system for each wavevector $\mathbf{k}$ when using the D2Q5 lattice show in Fig. 1, The linear systems for different wavenumbers are independent, and so can be solved in parallel.

The conserved moments of the f_i and $\mathbf{g}_i$ given by this procedure do not exactly match the conserved moments of the $f_i^{(0)}$ and $\mathbf{g}_i^{(0)}$, due to the coupling with adjacent lattice points. However, they differed by less than 1% in the numerical experiments. The reference solutions were initialised using the actual fields on the lattice after the initialisation of the lattice Boltzmann scheme by this procedure.

References

[1] J. U. Brackbill and D. C. Barnes. The effect of nonzero $\nabla\cdot\mathbf{B}$ on the numerical solution of the magnetohydrodynamic equations. *J. Comput. Phys.*, 35:426–430, 1980.

[2] D. Balsara and D. Spicer. Maintaining pressure positivity in magnetohydrodynamic simulations. *J. Comput. Phys.*, 148:133–148, 1999.

[3] G. Tóth. The $\nabla\cdot\mathbf{B}=0$ constraint in shock-capturing magnetohydrodynamics codes. *J. Comput. Phys.*, 161:605–652, 2000.

[4] D. J. Price and J. J. Monaghan. Smoothed particle magnetohydrodynamics - III. Multidimensional tests and the $\nabla\cdot\mathbf{B}=0$ constraint. *Mon. Not. Roy. Astron. Soc.*, 364:384–406, 2005.

[5] J. P. Boris. Relativistic plasma simulation – optimization of a hybrid code. In J. P. Boris and R. A. Shanny, editors, *Proceedings of the 4th Conference on Numerical Simulation of Plasmas*, pages 3–67, Washington, DC, 1972. Naval Research Laboratory.

[6] F. Assous, P. Degond, E. Heintze, P. A. Raviart, and J. Segre. On a finite-element method for solving the three-dimensional Maxwell equations. *J. Comput. Phys.*, 109:222–237, 1993.

[7] C.-D. Munz, R. Schneider, E. Sonnendrücker, and U. Voss. Maxwell's equations when the charge conservation is not satisfied. *C. R. Acad. Sci. I-Math.*, 328:431–436, 1999.

[8] F. Kemm, C.-D. Munz, R. Schneider, and E. Sonnendrücker. Divergence corrections in the numerical simulation of electromagnetic wave propagation. In H. Freistühler and G. Warnecke, editors, *Hyperbolic Problems: Theory, Numerics, Applications*, pages 603–612, Basel, 2001. Birkhäuser.

[9] K. Yee. Numerical solution of initial boundary value problems involving Maxwell's equations in isotropic media. *IEEE Trans. Antennas Propag.*, 14:302–307, 1966.

[10] C. R. Evans and J. F. Hawley. Simulation of magnetohydrodynamic flows – A constrained transport method. *Astrophys. J.*, 332:659–677, 1988.

[11] C. R. DeVore. Flux-corrected transport techniques for multidimensional compressible magnetohydrodynamics. *J. Comput. Phys.*, 92:142–160, 1991.

[12] J. M. Hyman and M. Shashkov. Mimetic discretizations for Maxwell's equations. *J. Comput. Phys.*, 151:881–909, 1999.

[13] K. Lipnikov, G. Manzini, and M. Shashkov. Mimetic finite difference method. *J. Comput. Phys.*, 257:1163–1227, 2014.
[14] A. J. Chorin. The numerical solution of the Navier–Stokes equations for an incompressible fluid. *Bull. Amer. Math. Soc.*, 73:928–931, 1967.
[15] A. J. Chorin. Numerical solution of the Navier–Stokes equations. *Math. Comp.*, 22:745–762, 1968.
[16] R. Témam. Sur l'approximation de la solution des équations de Navier–Stokes par la méthode des pas fractionnaires (II). *Arch. Ration. Mech. An.*, 33:377–385, 1969.
[17] A. L. Zachary, A. Malagoli, and P. Colella. A higher-order Godunov method for multidimensional ideal magnetohydrodynamics. *SIAM J. Sci. Comput.*, 15:263–284, 1994.
[18] A. Dedner, F. Kemm, D. Kroner, C. D. Munz, T. Schnitzer, and M. Wesenberg. Hyperbolic divergence cleaning for the MHD equations. *J. Comput. Phys.*, 175:645–673, 2002.
[19] A. J. Chorin. A numerical method for solving incompressible viscous flow problems. *J. Comput. Phys.*, 2:12–26, 1967.
[20] T. S. Tricco and D. J. Price. Constrained hyperbolic divergence cleaning for smoothed particle magnetohydrodynamics. *J. Comput. Phys.*, 231:7214–7236, 2012.
[21] H. Baty, F. Drui, E. Franck, P. Helluy, C. Klingenberg, and L. Tannhäuser. A kinetic method for solving the MHD equations. Application to the computation of tilt instability on uniform fine meshes. Preprint available from `https://hal.inria.fr/hal-02965967v1`, 2020.
[22] P. J. Dellar. Lattice kinetic schemes for magnetohydrodynamics. *J. Comput. Phys.*, 179:95–126, 2002.
[23] P. J. Dellar. Moment equations for magnetohydrodynamics. *J. Statist. Mech.*, P06003, 2009.
[24] P. J. Dellar. Electromagnetic waves in lattice Boltzmann magnetohydrodynamics. *Europhys. Lett.*, 90:50002, 2010.
[25] P. J. Dellar. Lattice Boltzmann magnetohydrodynamics with current-dependent resistivity. *J. Comput. Phys.*, 237:115–131, 2013.
[26] J. Zhao. Discrete-velocity vector-BGK models based numerical methods for the incompressible Navier–Stokes equations. *Commun. Comput. Phys.*, 29:420–444, 2021.
[27] L. D. Landau and E. M. Lifshitz. *Classical Theory of Fields*. Pergamon, Oxford, 4th edition, 1975.
[28] J. D. Jackson. *Classical Electrodynamics*. Wiley, New York, 3rd edition, 1999.
[29] D. Biskamp. *Nonlinear Magnetohydrodynamics*. Cambridge University Press, Cambridge, 1993.
[30] W. Rindler. *Introduction to Special Relativity*. Oxford University Press, Oxford, 1982.
[31] P. Janhunen. A positive conservative method for magnetohydrodynamics based on HLL and Roe methods. *J. Comput. Phys.*, 160:649–661, 2000.
[32] K. G. Powell. An approximate Riemann solver for magnetohydrodynamics (that works in more than one dimension). ICASE Report No. 94-24, NASA Langley Research Center, 1994. Available from `http://hdl.handle.net/2060/19940028527`.
[33] K. G. Powell, P. L. Roe, T. J. Linde, T. I. Gombosi, and D. L. De Zeeuw. A solution-adaptive upwind scheme for ideal magnetohydrodynamics. *J. Comput. Phys.*, 154:284–309, 1999.
[34] S. K. Godunov. Symmetric form of the equations of magnetohydrodynamics. *Chislennye Metody Mekh. Sploshnoi Sredy*, 1:26–34, 1972, in Russian.
[35] Y. H. Qian, D. d'Humières, and P. Lallemand. Lattice BGK models for the Navier–Stokes equation. *Europhys. Lett.*, 17:479–484, 1992.
[36] S. Succi. *The Lattice Boltzmann Equation: For Complex States of Flowing Matter*. Oxford University Press, Oxford, 2018.

[37] P. Lallemand, L.-S. Luo, M. Krafczyk, and W.-A. Yong. The lattice Boltzmann method for nearly incompressible flows. *J. Comput. Phys.*, 431:109713, 2021.
[38] X. He, S. Chen, and G. D. Doolen. A novel thermal model of the lattice Boltzmann method in incompressible limit. *J. Comput. Phys.*, 146:282–300, 1998.
[39] P. J. Dellar. Incompressible limits of lattice Boltzmann equations using multiple relaxation times. *J. Comput. Phys.*, 190:351–370, 2003.
[40] P. L. Bhatnagar, E. P. Gross, and M. Krook. A model for collision processes in gases. I. Small amplitude processes in charged and neutral one-component system. *Phys. Rev.*, 94:511–525, 1954.
[41] M. Hénon. Viscosity of a lattice gas. *Complex Sys.*, 1:763–789, 1987.
[42] G. Strang. On the construction and comparison of difference schemes. *SIAM J. Numer. Anal.*, 5:506–517, 1968.
[43] P. J. Dellar. An interpretation and derivation of the lattice Boltzmann method using Strang splitting. *Comput. Math. Applic.*, 65:129–141, 2013.
[44] Y. H. Qian and S. A. Orszag. Lattice BGK models for the Navier-Stokes equation: Nonlinear deviation in compressible regimes. *Europhys. Lett.*, 21:255–259, 1993.
[45] S. Hou, Q. Zou, S. Chen, G. D. Doolen, and A. C. Cogley. Simulation of cavity flow by the lattice Boltzmann method. *J. Comput. Phys.*, 118:329–347, 1995.
[46] H. Helmholtz. Über Integrale der hydrodynamischen Gleichungen, welche den Wirbelbewegungen entsprechen. *J. Reine Angew. Math.*, 1858:25–55, 1858.
[47] A. J. Chorin and J. E. Marsden. *A Mathematical Introduction to Fluid Mechanics*. Springer, 1993.
[48] H. Jeffreys. *The Earth*. Cambridge University Press, Cambridge, 1929.
[49] R. B. Bird, R. C. Armstrong, and O. Hassager. *Dynamics of Polymeric Liquids*, volume 1. Wiley, New York; Chichester, 2nd edition, 1987.
[50] J. G. Oldroyd. On the formulation of rheological equations of state. *Proc. R. Soc. Lond. A*, 200:523–541, 1950.
[51] E. Anderson et al. *LAPACK Users' Guide*. SIAM, Philadelphia, 3rd edition, 1999.
[52] M. Frigo and S. G. Johnson. The design and implementation of FFTW3. *Proc. IEEE*, 93:216–231, 2005.
[53] A. Richards. University of Oxford Advanced Research Computing. Technical Note `https://doi.org/10.5281/zenodo.22558`, 2015.